Bone Microstructure of Pareiasaurs (Parareptilia) from the Karoo Basin, South Africa: Implications for Growth Strategies and Lifestyle Habits

AURORE CANOVILLE* AND ANUSUYA CHINSAMY
[1]Department of Biological Sciences, University of Cape Town, Private Bag X3, Rondebosch, 7701, South Africa

ABSTRACT

Numerous morphological studies have been carried out on pareiasaurs; yet their taxonomy and biology remain incompletely understood. Earlier works have suggested that these herbivorous parareptiles had a short juvenile period as compared to the duration of adulthood. Several studies further suggested an (semi-) aquatic lifestyle for these animals, but more recent investigations have proposed a rather terrestrial habitat. Bone paleohistology is regarded as a powerful tool to assess aspects of tetrapod paleobiology, but few studies have been conducted on pareiasaurs. The present study assesses intra and inter-specific histovariability of pareiasaurs and provides fresh insights into their paleobiology, thereby permitting a re-evaluation of earlier hypotheses. Our sample comprises various skeletal elements and several specimens covering most of the taxonomic and stratigraphic spectrum of South African pareiasaurs, including large and basal forms from the Middle Permian, as well as smaller and more derived forms from the Late Permian. Our results concerning size of elements and histological tissues show that for pareiasaurs, element size is not a good indicator of ontogenetic age, and furthermore, suggest that the specific diversity of the Middle Permian pareiasaurs may have been underestimated. The bone histology of these animals shows that they experienced a relatively rapid growth early in ontogeny. Periosteal growth later slowed down, but seems to have been protracted for several years during adulthood. Pareiasaur bone microanatomy is unusual for continental tetrapods, in having spongious stylopod diaphyses and thin compact cortices. Rigorous paleoecological interpretations are thus limited since no modern analogue exists for these animals. Anat Rec, 300:1039–1066, 2017. © 2016 Wiley Periodicals, Inc.

Key words: bone histology; lifestyle adaptation; bone core drilling; growth pattern; taxonomy; *Tapinocephalus* assemblage zone

Grant sponsors: Claude Leon Foundation, South Africa; National Research Foundation, South Africa.

Present address: Aurore Canoville, Steinmann Institute for Geology, Mineralogy, Paleontology, University of Bonn, Nußallee 8, Bonn 53115, Germany.

*Correspondence to: Aurore Canoville, Department of Biological Sciences, University of Cape Town, Private Bag X3, Rondebosch, 7701, South Africa. E-mail: canoville.aurore08@gmail.com

Received 31 August 2016; Revised 14 October 2016; Accepted 21 October 2016.

DOI 10.1002/ar.23534

Published online 20 December 2016 in Wiley Online Library (wileyonlinelibrary.com).

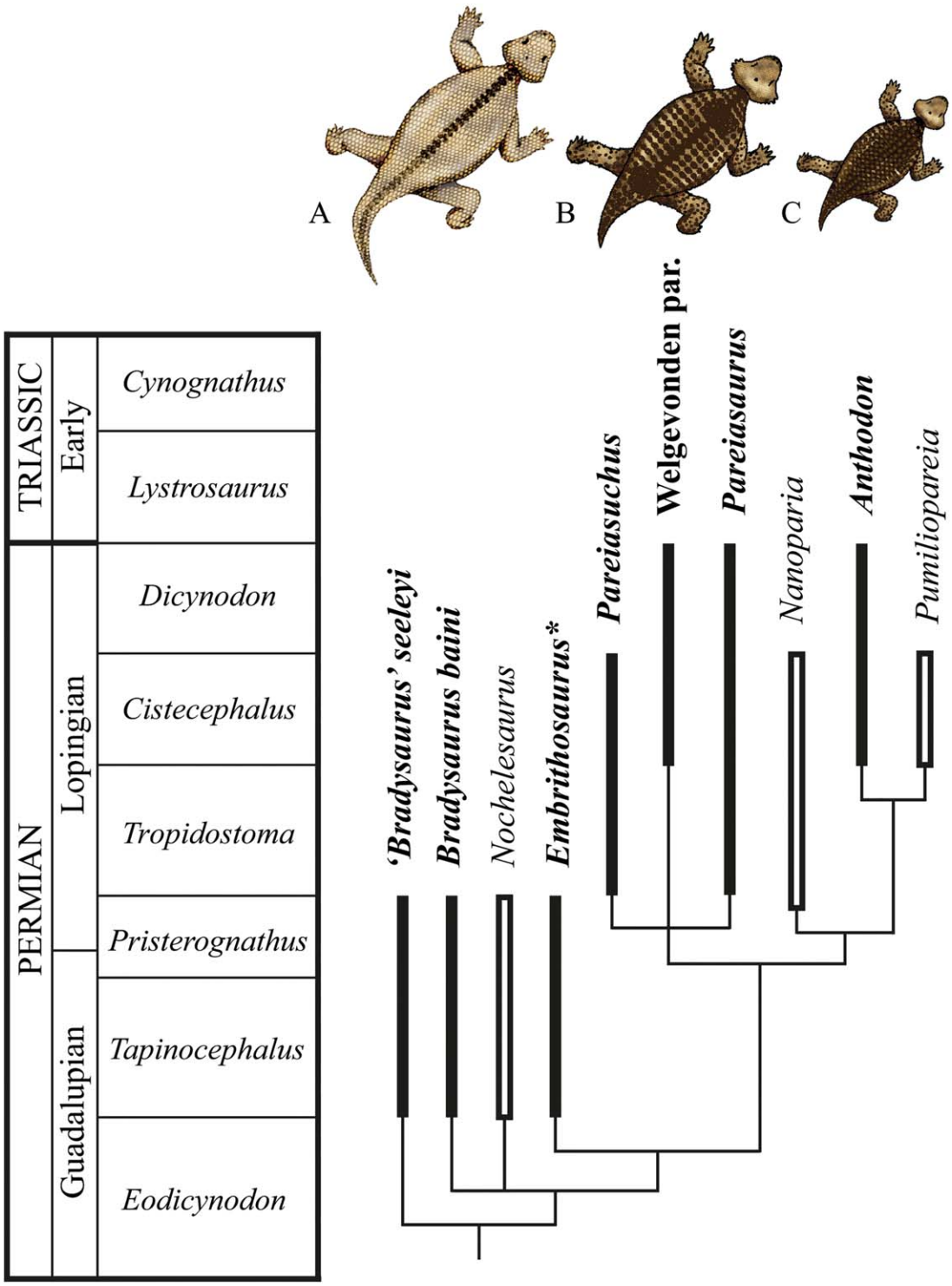

Fig. 1. Phylogeny of Southern African pareiasaurs. Modified from Lee (1997b) and Tsuji and Müller (2008). The genera sampled in the present study are highlighted in bold. The genus *Embrithosaurus* is marked with an asterisk because, during his taxonomic revision of Pareiasauria, Lee (1997a) considered that most of the specimens described as *Embrithosaurus* in the museum's collections (apart from few referred specimens) were not clearly distinguishable from the genus *Bradysaurus*. Both specimens sampled in the present study were not listed as referred specimens by Lee (1997a). Thus, the taxonomic identification of these specimens has to be considered cautiously. The stratigraphic range for each taxon reflects a consensus of the data found in the literature (Table 1). The Welgevonden pareiasaur (Welgevonden par.) corresponds to the specimen SAM-PK-1058, which constitutes a new species of pareiasaur according to Lee (1997a). **A**–**C**: the different morphotypes of South African pareiasaurs [modified from Lee (1997a) and Scheyer and Sander (2009)]. A: large pareiasaurs with a small dermal armour composed of isolated osteoderms restricted to a narrow band above the vertebral column (such as *Bradysaurus*, *Embrithosaurus* and *Nochelesaurus*); B: medium to large-sized pareiasaurs with mostly isolated osteoderms covering the complete body (such as *Pareiasaurus*, *Pareiasuchus* and the Welgevonden pareiasaur, SAM-PK-1058); C: dwarf, highly derived forms with osteoderms covering the complete body and united into a dorsal carapace (such as *Anthodon*, *Pumiliopareia*, and *Nanoparia*).

TABLE 1. Stratigraphic range of the valid South African pareiasaur genera and species according to different sources in the literature

	Stratigraphic range					
Genus/species	Lee (1997a)	Jalil and Janvier (2005)	Nicolas and Rubidge (2010)	Tsuji (2011)	Smith et al. (2012)	Day et al. (2015)
Bradysaurus seeleyi	*Tapino.*	*Tapino., Pristero.*	*Tapino.*	*Tapino., Pristero.*	*Tapino., Pristero.*	*Tapino.*
Bradysaurus baini	*Tapino.*	*Tapino., Pristero.*	*Tapino.*	*Tapino., Pristero.*	*Tapino., Pristero.*	*Tapino.*
Nochelesaurus	*Tapino.*	*Tapino., Pristero.*	*Tapino.*	*Tapino.*	*Tapino.*	*Tapino.*
Embrithosaurus	*Tapino.*	*Tapino., Pristero.*	*Tapino.*	*Tapino.*	*Tapino., Pristero.*	*Tapino.*
Pareiasuchus	*Ciste.*	*Trop., Ciste.*	*Ciste.*	–	–	–
Pareiasaurus	*Ciste., Dapto.*	*Trop., Ciste., Dicyn.*	*Trop., Ciste., Dicyn.*	*Trop., Ciste., Dicyn.*	*Trop., Ciste., Dicyn.*	*Trop.*
Welgevonden pareiasaur	*Ciste., Dapto.*	*Trop.? Ciste.? Dicyn.?*	–	*Ciste., Dapto.*	–	–
Nanoparia	*Ciste.*	*Trop., Ciste.*	*Ciste.*	*Ciste.*	*Ciste.*	–
Anthodon	*Ciste.*	*Ciste.*	*Ciste.*	*Ciste.*	*Ciste., Dicyn.*	–
Pumiliopareia	*Ciste.*	*Ciste.*	–	*Ciste.*	–	–

Our Figure 1 represents a consensus of all these studies with the largest stratigraphic range taking into account for each taxa. The *Daptocephalus* AZ mentioned in Lee (1997a) corresponds to the *Dicynodon* AZ (Rubidge et al., 1995). Abbreviations, *Ciste.*: *Cistecephalus* AZ; *Dapto.*: *Daptocephalus* AZ; *Dicyn.*: *Dicynodon* AZ; *Pristero.*: *Pristerognathus* AZ; *Tapino.*: *Tapinocephalus* AZ; *Trop.*: *Tropidostoma* AZ.

Pareiasaurs (Parareptilia) constituted a prominent tetrapod group and included some of the largest herbivores (they ranged in length from 1 to 3.5 m in snout-vent length; Lee, 1997a) in the Middle and Late Permian continental ecosystems (Smith et al., 2012; Pearson et al., 2013). In less than 16 million years (from the Wordian to the end of the Changhsingian), they achieved a significant radiation with 21 recognized species and an extensive geographic distribution (Lee, 1997a; Tsuji, 2011, 2013; Turner et al., 2015; Benton, 2016). Their remains are common in South Africa and Russia and have been identified to a lesser extent in Brazil, China, Germany, Niger, Morocco, Scotland, Tanzania and Zambia (Tsuji, 2011). However, it is undisputed that pareiasaurs are most abundant and taxonomically diverse in the Karoo Basin of South Africa (8 genera, 10 to 11 species; Fig. 1; Lee, 1997a; Tsuji, 2011), and importantly, the study of Lee (1997a) implies several sympatric species. Three to four genera of South African pareiasaurs are believed to have co-existed within the *Tapinocephalus* Assemblage Zone (AZ), and up to six within the *Cistecephalus* AZ, implying various ecological adaptations among this group (Fig. 1; Lee, 1997a; Tsuji, 2011). Pareiasaurs suffered at least two episodes of extinctions, with a first phase of decline at the end of the Guadalupian (Lee, 1997a; Day et al., 2015), and then, at the end of the Permian when the last members of the clade perished (Lee, 1997a; Lee et al., 1997; Ruta et al., 2011).

Bereft of living descendants, Pareiasauria are a taxonomic vagrant, and their phylogenetic affinities among the Parareptilia have been long debated (Gregory, 1946; Lee, 1994a, 1996, 1997b; Laurin and Reisz, 1995; Tsuji, 2006; Tsuji and Müller, 2009; Tsuji et al., 2012). Even though these animals have been the subject of numerous anatomical and taxonomic studies since the 19th century (see Tsuji, 2011 for a review), their paleobiology is poorly known and reconstructing their life history traits has proven challenging. Thus, ontogenetic variability, growth strategies, and lifestyle habits of these herbivorous animals remain poorly understood. Earlier anatomical and taphonomic studies have suggested that pareiasaurs had a rather short juvenile period as compared to adulthood (Spencer and Lee, 2000, see also Turner et al., 2015), and that juveniles and adults may have occupied different habitats. Some authors also pointed out that little is known about the ontogenetic development of pareiasaurs since few juvenile specimens have been identified (Kordikova and Khlyupin, 2001) and that it may well be that so-called « dwarf pareiasaurs » (Lee, 1997b) could simply be juveniles (Tsuji, 2011).

Divergent lifestyle adaptations have been proposed for this group. Based on their massive body-size, stout limbs, and characteristic dentition, pareiasaurs have been hypothesized to be fully aquatic, dugong-like animals that fed on algae or plankton (Case, 1926; Hartmann-Weinberg, 1937; Ivakhnenko, 1987). Several researchers considered anatomical and taphonomic findings to suggest that pareiasaurs were semi-aquatic (hippo ecomorphs) or at least water-dependent for feeding, inhabiting swampy environments (Boonstra, 1955, 1969; Piveteau, 1955; Ochev, 1995, 2004; MacRae, 1999; Tverdokhlebov et al., 2005; Khlyupin, 2007; Sumin, 2009). Kriloff et al. (2008) reached similar deductions through bone microanatomical analyses, using an inference model built on the tibia of amniotes. Interestingly,

TABLE 2. Material sampled for histological study

Species/genus identification	Specimen no.	Collection	Locality	Assemblage zone (as reported in the museum's collections)	Skeletal element	Length (cm)	Section type
Bradysaurus seeleyi	SAM-PK-9137	SAM	Vogelfontein, Prince Albert	*Tapinocephalus*	Femur (R)	33.9	BC
					Tibia (R)	–	BC
					Fibula	–	CT
Bradysaurus seeleyi	SAM-PK-9165	SAM	Kruisvlei, Beaufort West	*Tapinocephalus*	Femur (L)	40.5	BC
Bradysaurus baini	SAM-PK-5127	SAM	Leeurivier, Beaufort West	*Tapinocephalus*	Femur (L)	45	BC
					Fibula 1 (R)	–	CT
					Fibula 2 (L)	–	CT
Bradysaurus baini	SAM-PK-3533	SAM	Hottentotsrivier, Beaufort West	*Tapinocephalus*	Rib 1 (MT)	5.9	CT
					Rib 2 (MT)	9.6	CT
Bradysaurus sp.	SAM-PK-12057	SAM	Leeuwkraal, Beaufort West	*Tapinocephalus*	Femur (R)	22.2	BC
					Tibia (R)	16.7	BC
Bradysaurus sp.	SAM-PK-12129	SAM	Wilgerfontein, Prince Albert	*Tapinocephalus*	Femur (L)	24.2	BC
Bradysaurus sp.	SAM-PK-9355	SAM	Roggekloof, Sutherland	*Tapinocephalus*	Femur (L)	28.6	BC
Bradysaurus sp.	SAM-PK-12047	SAM	Klipfontein, Laingsburg	*Tapinocephalus*	Radius (L)	–	BC
Bradysaurus sp.	BP/I/5430	ESI	Swaerskraal, Laingsburg	*Tapinocephalus*	Fibula	–	CT
Embrithosaurus sp.[a]	SAM-PK-9116	SAM	Vogelfontein, Prince Albert	*Tapinocephalus*	Femur (R)	30.8	BC
					Radius (?)	20.9	BC
Embrithosaurus sp.[a]	SAM-PK-9128	SAM	Vogelfontein, Prince Albert	*Tapinocephalus*	Radius (L)	–	CT
					Fibula (L)	–	CT
Pareiasaurus sp.	BP/I/5282	ESI	Modderfontein, Victoria West	*Cistecephalus*	Femur (R)	22	CT
Pareiasaurus serridens	SAM-PK-10032	SAM	Swaelkrantz, Murraysburg	*Dicynodon*	Femur (L)	32	BC
					Tibia (L)	18.0	BC
The Welgevonden pareiasaur	SAM-PK-1058	SAM	Welgevonden, Graaff-Reinet	*Tropidostoma*	Humerus (R)	–	BC
					Ribs	–	CT
Pareiasuchus nasicornis	SAM-PK-K6607	SAM	Amandelboom, Fraserburg	*Tropidostoma* / *Cistecephalus?*	Tibia (R)	–	BC
					Rib (MT)	10.4	CT
Anthodon serrarius	SAM-PK-10074	SAM	Dunedin, Beaufort West	Upper *Tropidostoma* / Lower *Cistecephalus?*	Femur (L)	20.5[b]	BC
					Fibula (L)	8.88	CT
Anthodon serrarius	SAM-PK-10026	SAM	Klein Bloemhof, Richmond	*Dicynodon*	Rib (MT)	–	CT
Anthodon serrarius	BP/I/548	ESI	–	Lower Upper *Cistecephalus*	Rib	–	CT
Pareiasauria Indet.[c]	SAM-PK-4996	SAM	Leeu Gamka, Prince Albert	*Tapinocephalus*	Femur (R)	26.3	BC
Pareiasauria Indet.[c]	SAM-PK-4344	SAM	Wolwefontein, Prince Albert	*Tapinocephalus*	Femur (R)	26.3	BC
Pareiasauria Indet.[c]	SAM-PK-K322	SAM	Morewag, Beaufort West	*Tapinocephalus*	Femur (R)	33.3	BC
					Tibia (R)	21.1	BC
Pareiasauria Indet.[c]	BP/I/347	ESI	Buffelsvlei, Merweville	*Tapinocephalus*	Rib 1 (MT)	–	CT
					Rib 2 (MT)	–	CT
					Rib 3 (MT)	–	CT
					Rib 4 (MT)	–	CT

TABLE 2. (continued).

Species/genus identification	Specimen no.	Collection	Locality	Assemblage zone (as reported in the museum's collections)	Skeletal element	Length (cm)	Section type
Pareiasauria Indet.[c]	BP/I/1574	ESI	De Bad, Fraserburg	*Tapinocephalus*	Rib 1 (MT)	–	CT
					Rib 2 (MT)	–	CT
					Fibula (?)	–	CT
Pareiasauria Indet.[c]	SAM-PK-6554	SAM	Abrahamskraal, Prince Albert	*Tapinocephalus*	Rib (MT)	5.95	CT
Pareiasauria Indet.[c]	SAM-PK-8948	SAM	Mynhardtskraal, Beaufort West	*Tapinocephalus*	Fibula (?)	–	CT

All the material comes from the Karoo Basin, South Africa. Abbreviations: ESI, Evolutionary Studies Institute, University of the Witwatersrand, Johannesburg (formerly the Bernard Price Institute for palaeontology - BPI); SAM, Iziko South African Museum, Cape Town; R, Right; L, Left; MT, mid-thoracic; ?, unidentifiable; BC, Bone Core; CT, Cross-section.

[a]During his taxonomic revision of Pareiasauria, Lee (1997a) considered that most of the specimens described as *Embrithosaurus* in the museum's collections (apart from few referred specimens) were not clearly distinguishable from the genus *Bradysaurus*. Both specimens sampled in these study are not listed as referred specimens in Lee (1997a). Thus, the taxonomic identification of these specimens has to be considered cautiously.

[b]Size extrapolated by Boonstra (1932).

[c]These specimens were assigned to the *Pareiasaurus* genus in the museum's collections. They have all been recovered from the *Tapinocephalus* AZ. However, according to the literature, the earliest record for the *Pareiasaurus* genus is from the *Tropidostoma* AZ (see Table 1). These specimens are thus considered as Pareiasauria Indet. in the present study.

pareiasaurs have usually been found in flood plain and lake deposits, sometimes in association with other aquatic or semi-aquatic vertebrates such as fishes, temnospondyls, and chroniosuchids (Tverdokhlebov et al., 2005). Moreover, specimens of *Bradysaurus* (South Africa) and *Deltavjatia* (Russia) are frequently discovered as complete articulated skeletons, sometimes preserved in upright positions, suggesting that they may have been trapped in mud (Boonstra, 1969; Ochev, 1995; MacRae, 1999). Contrarily, some authors suggested that pareiasaurs were fully terrestrial browsers (Lee, 1994a,b; Benton et al., 2004, 2012; Canoville et al., 2014; Smith et al., 2015; Turner et al., 2015). Such interpretations mostly rely on pareiasaurs limb anatomy and the recovery of numerous footprints attributed to this group (Gubin et al., 2003; Valentini et al., 2009; Voigt et al., 2010; Turner et al., 2015). Moreover, a preliminary stable light isotope analysis by Canoville et al. (2014) suggested that Middle Permian pareiasaurs from the Karoo Basin lived in a terrestrial habitat. A more recent and extensive isotopic study (Rey et al., 2015) has confirmed that pareiasaurs from the *Tapinocephalus* AZ had a terrestrial lifestyle. However, Rey et al. (2015) also found that more derived pareiasaurs from the Upper Permian had isotopic values that suggested a rather semi-aquatic to aquatic lifestyle.

When gross-morphology and taphonomy offer limited or equivocal information to infer the paleo-biology and ecology of extinct taxa, bone microstructure can provide insight into the ontogenetic stage, individual age, growth pattern, and ecology of these groups (Castanet et al., 2001; Chinsamy-Turan, 2005, 2012; Ricqlès, 2011; Padian and Lamm, 2013). Although bone microstructural analyses have been extensively applied to the diverse and abundant non-mammalian therapsids from the Karoo Basin, South Africa (e.g., Chinsamy and Rubidge, 1993; Botha and Chinsamy, 2005; Ray et al., 2009; Botha-Brink and Angielczyk, 2010; Chinsamy-Turan, 2012; Jasinoski and Chinsamy, 2012; Nasterlack et al., 2012) only a few studies have been conducted on parareptiles (Ricqlès, 1974; Scheyer et al., 2010; Botha-Brink and Smith, 2012; Lyson et al., 2013, 2014; Tsuji et al., 2015; Looy et al., 2016). Some of these studies have assessed pareiasaur bone microstructure and these have been on rather limited samples (Ricqlès, 1974, 1976a,b; Kriloff et al., 2008; Scheyer and Sander, 2009; Lyson et al., 2013, 2014; Tsuji et al., 2015; Looy et al., 2016). Armand de Ricqlès was the first to study pareiasaur bone histology (1974, 1976a,b). He sampled bone fragments of two genera of pareiasaurs, namely *Bradysaurus* sp. and *Pareiasaurus serridens*, and reported that the long bone diaphysis of both genera comprised « lamellar-zonal » bone tissue with moderate to highly vascularized zones and thin avascular annuli, suggesting a rather high, but cyclical bone depositional rate (Ricqlès, 1978). Perimedullar remodeling was reported as being extensive in the limb bones and the medullary cavities were usually infilled extensively with spongiosa. Ricqlès (1974) however, found that the rib structure was different and showed extensive Haversian remodeling and a medullary region with or without bone trabeculae.

To reassess previous hypotheses pertaining to the biology and ecology of pareiasaurs, we undertake a comprehensive survey of pareiasaurian long bone histology and microanatomy through the examination of a large

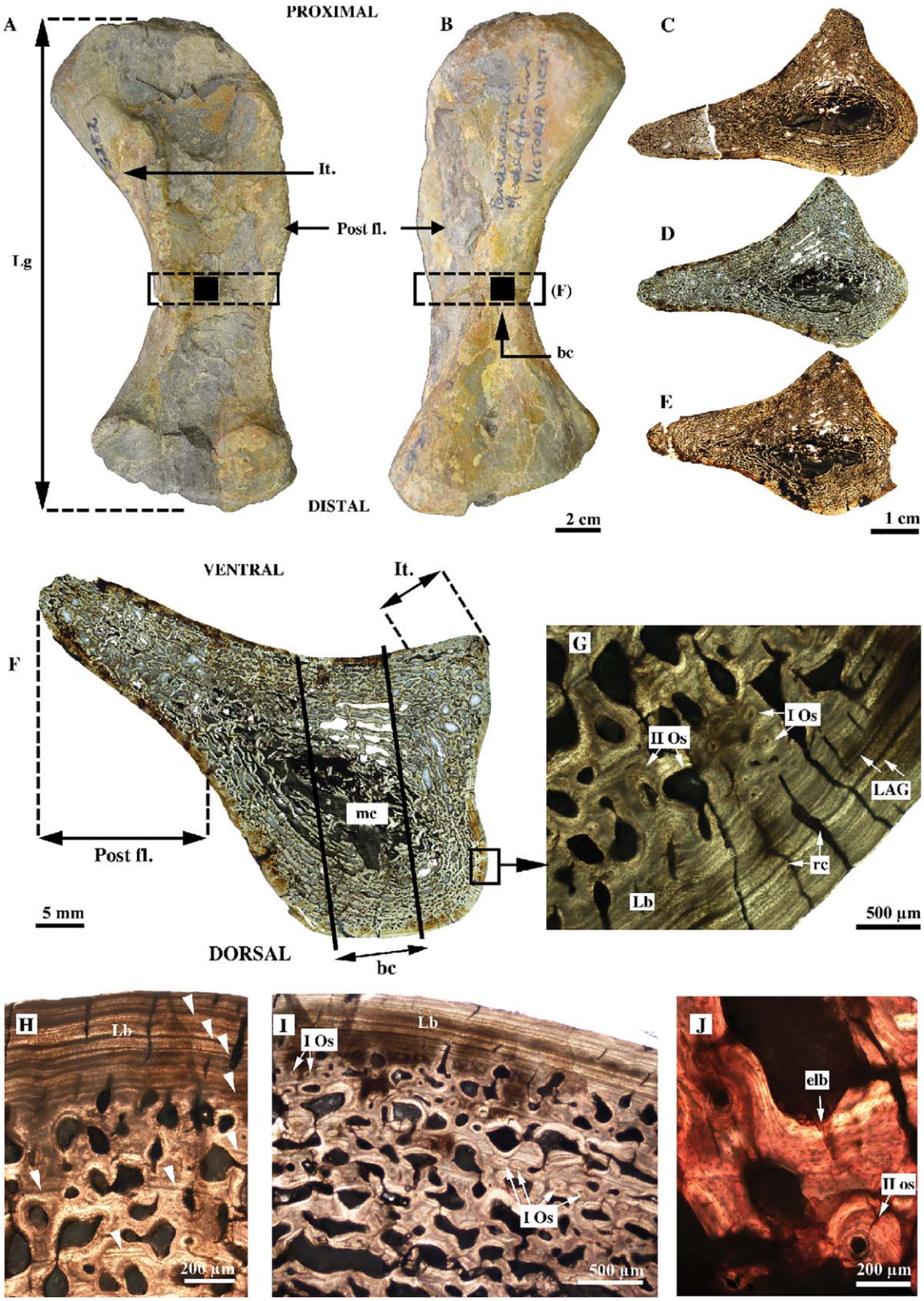
A
PROXIMAL
It.
Post fl.
Lg
DISTAL
B
(F)
bc
2 cm
C
D
E
1 cm
VENTRAL
It.
F
mc
Post fl.
5 mm
DORSAL
bc
G
I Os
II Os
LAG
rc
Lb
500 µm
H
Lb
200 µm
I
Lb
I Os
I Os
500 µm
J
elb
II os
200 µm

Fig. 2.

number of taxa and diverse skeletal elements, from different stratigraphic horizons, as well as differing body sizes.

MATERIAL AND METHODS

Sample

General considerations on South African pareiasaur taxonomy and stratigraphic range. The most recent taxonomic revisions available for this clade have been carried out by Lee (1997a) and Tsuji (2011). Among South African pareiasaurs from the Karoo Basin, these authors recognize eight to nine valid genera comprising 10–11 species (the Welgevonden pareiasaur being a new species, and maybe a new genus, according to Lee (1997a; Fig. 1). Nevertheless, the taxonomy and the diversity of South African pareiasaurs remain complex and are still incompletely understood. A possible new species of pareiasaur from the *Tapinocephalus* AZ of South Africa has been mentioned recently (Cisneros and Rubidge, 2012). Moreover, a large amount of pareiasaur material is available in museum collections, with several recently discovered specimens that have not been considered by Lee (1997a) in the course of his taxonomic revision and would require new in depth anatomical studies to be referred to their correct taxa (Nicolas, 2007; Tsuji and Müller, 2008; Tsuji, 2011; first author personal observation, 2013).

The stratigraphic range of some South African genera is also controversial in the literature (Table 1). Our time-calibrated phylogeny (Fig. 1) thus results from a consensus of Lee (1997a), Jalil and Janvier (2005), Nicolas and Rubidge (2010), Tsuji (2011), Smith et al. (2012), and Day et al. (2015). For example, specimen SAM-PK-10074 identified as *Anthodon serrarius* and described as such in Boonstra (1932) and Lee (1997a) is catalogued from the *Tropidostoma* AZ in the collections of the Iziko South African Museum, Cape Town, even though the genus is described as restricted to the *Cistecephalus* and the *Dicynodon* AZ in the literature (Boonstra, 1932; Lee, 1997a; Nicolas, 2007). It is likely that the stratigraphic information recorded for this specimen in the museum's collection is incorrect and we have relied on the published data. It is also worth noting that the *Daptocephalus* AZ mentioned in earlier studies (e.g., Lee, 1997a) corresponds to the *Dicynodon* AZ (Rubidge et al., 1995).

We are aware that misidentifications may exist in the museum's database, and we recognized seven specimens from our sample as misidentified at the generic level (specimens SAM-PK-4996, SAM-PK-4344, SAM-PK-K322, BP/I/347, BP/I/1574, SAM-PK-6554, SAM-PK-8948; Table 2). Indeed, they were collected in localities corresponding to the *Tapinocephalus* AZ, but were previously assigned to the genus *Pareiasaurus* sp., which according to the literature, is not found in deposits predating the *Tropidostoma* AZ (Table 1; Fig. 1). These specimens, marked as Pareiasauria indet. in Table 1, could be related to the large, basal pareiasaurian genera such as *Bradysaurus*, *Embrithosaurus*, or *Nochelesaurus* or could even represent new undescribed taxa. A recent study of the taxonomic diversity of the *Tapinocephalus* AZ highlights the fact that more than 50% of the pareiasaurian remains are not identified at the generic level in South African museum collections (Smith et al., 2012; Table 2). Moreover, during his taxonomic revision of Pareiasauria, Lee (1997a) noted that most of the specimens described as *Embrithosaurus* in the museums' collections (apart from a few referred specimens) were not readily distinguishable from the genus *Bradysaurus*. Both specimens sampled in these study are not listed as referred specimens in Lee (1997a). Thus, the taxonomic identification of these specimens has to be considered with caution.

Taxonomic diversity of the studied sample. Our sample is representative of the broad morphological and stratigraphic diversity of South African pareiasaurs. It includes, (i) some of the most basal and also earliest known pareiasaurs, such as *Bradysaurus*. This form represents large pareiasaurs up to 2.5 m in snout-vent length with a small dermal armor composed of isolated osteoderms restricted to a narrow band above the vertebral column (Lee, 1997a; Fig. 1A); (ii) medium sized to large intermediate forms, such as the genera *Pareiasuchus* and *Pareiasaurus* (snout-vent lengths of 2–2.5 m). These animals exhibited mostly isolated osteoderms covering the complete body (Lee, 1997a; Lee et al., 1997; Fig. 1B); (iii) dwarf, highly derived forms, such as the genus *Anthodon*, with a body size around one meter in snout-vent length and osteoderms covering the complete body which are united into a dorsal carapace (Fig. 1C).

Fig. 2. The different levels of integration of a limb bone in the present study. Example of the right femur of specimen *Pareiasaurus* sp. BP/I/5282. Anatomical level (**A**, **B**); microanatomical level (**C**–**F**); histological level (**G**–**J**). A: Ventral view of the femur. B: dorsal view of the femur. The maximal length (Lg) of the femur is 22 cm. The dotted rectangle represents the mid-shaft region where the complete cross-section (D, F) has been done. The black square indicates the standardized zone where the bone cores have been sampled for all other femora (Table 2). C: Cross-section of the proximal metaphysis. D: cross-section of the mid-shaft. E: Cross-section of the distal metaphysis. F: cross-section of the mid-diaphysis (maximal diameter: 56 mm). This cross-section, typical of a pareiasaurian femur, allowed identifying the most suitable location to sample the bone cores (away from the postaxial flange and the internal trochanter). G: Detail of F showing the extent of remodeling in the cortex. The oldest primary osteons are slowly changed by erosion and reconstruction processes into secondary osteons. Many of these secondary osteons are not complete and retain a wide Haversian canal. By this process, the deepest part of the primary cortex is progressively changed into a spongiosa. The outermost cortex is formed by a slowly deposited lamellar bone interrupted by lines of arrested growth (LAGs). Even though this outer layer is poorly vascularized, it contains few simple radial canals. H: The middle cortex is highly remodeled but few island of primary bone are still visible. The primary bone is formed of a lamellar-zonal bone tissue interrupted by growth marks (arrow heads). The spacing between the growth marks seems to decrease toward the bone surface together with bone vascularization. I: Rows of small primary osteons are still visible in the mid-cortex that is progressively remodeled by Haversian substitution. J: Close-up of bone trabeculae in the deep cancellous cortical bone. These trabeculae are mostly formed by lining of endosteal lamellar bone. Abbreviations: bc, bone core; elb, endosteal lamellar bone; It, internal trochanter; LAG, line of arrested growth; Lb, lamellar bone; Lg, maximal length; mc, medullary cavity; rc, radial canal; I Os, primary osteons; II Os, secondary osteons; Post fl, postaxial flange.

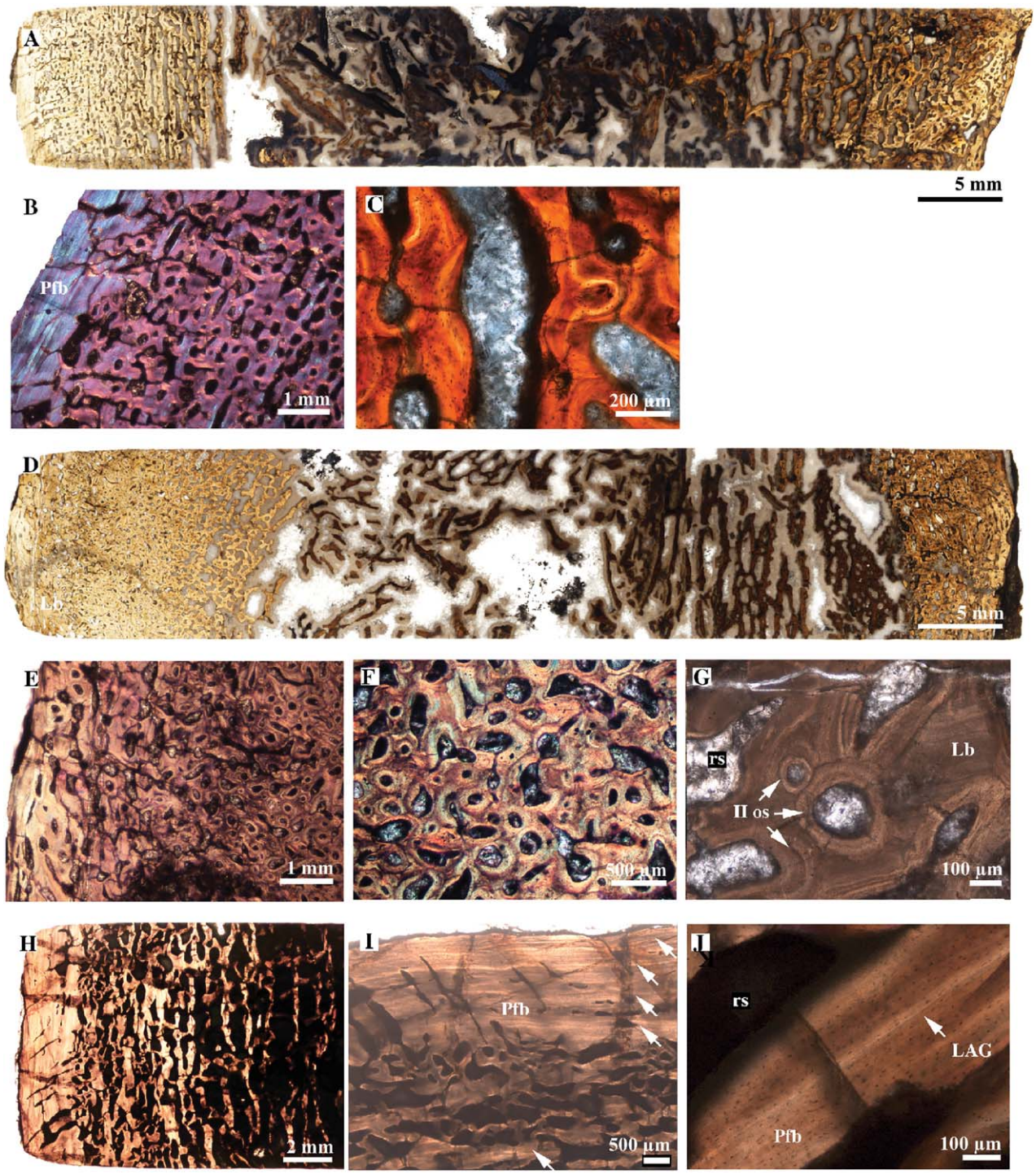

Fig. 3. Long bone microstructure of the large pareiasaur specimens identified as *Bradysaurus seeleyi*. **A**: Bone core of the femur of specimen SAM-PK-9137 (dorsal side to the left; ventral side to the right; length: 60 mm). **B**: Cortex on the dorsal side (detail from A). Most of the inner cortex has been remodeled and is formed of incipient secondary osteons and resorption spaces lined by endosteal bone (polarized light). **C**: Secondary bone trabeculae in the perimedullary region of the femur in A. **D**: Bone core of the tibia of specimen SAM-PK-9137 (dorsal side to the left; ventral side to the right; length: 53.2 mm). **E**: Detail of the outermost cortex on the dorsal side of the tibia in D. Note the change in organization of the bone tissue towards the periphery with decrease in bone remodeling and vascularization suggesting a slow down of growth. **F**: Detail of the mid-cortex on the dorsal side of the tibia in D. **G**: close up in the outer cortex showing several generations of secondary osteons and large resorption spaces with lining of endosteal lamellar bone. Some remnants of primary lamellar bone are visible in the interstitial spaces. **H**: Dorsal side of the bone core sampled on the femur of specimen SAM-PK-9165. **I**: Detail of the outer cortex of the femur in H. The vascularization decreases and the parallel-fibered bone matrix becomes more lamellar towards the bone surface. The arrows point at evenly spaced LAGs. **J**: Detail of a preserved patch of primary parallel-fibered bone with a LAG in the mid-cortex of the femur in H. Abbreviations: LAG, line of arrested growth; Lb, lamellar bone; Pfb, parallel-fibered bone; rs, resorption space; II os, secondary osteon.

The large form *Nochelesaurus alexanderi* from the *Tapinocephalus* AZ was not selected for our study because the validity of this genus has been contested and little material was available for thin-sectioning. According to Lee (1997a), the few specimens described as *Nochelesaurus* are very similar to *Bradysaurus*. For the dwarf genera *Nanoparia* and *Pumiliopareia* very few postcranial elements are known (Lee, 1997a), and they were therefore not included in our study.

Skeletal elements and ontogenetic stages sampled. In the present study, we were permitted to sample broken, incomplete or taphonomically distorted skeletal elements with limited public display value (Table 2). Limb bones were preferentially used as they exhibit the least secondary remodeling in the midshaft region compared to other skeletal elements, and they are considered to provide the best record of the primary bone tissue (Francillon-Vieillot et al., 1990; Chinsamy-Turan, 2012). We also sampled ribs because of their general abundance in the collections, and since non-weight bearing bones (e.g., fibula, ribs) may exhibit a better growth mark record than weight bearing bones (Stein and Sander, 2009; Waskow and Sander, 2014).

To document growth patterns, and intra- and interspecific bone histovariability of these animals, our study examines 43 skeletal elements (femora, humeri, radii, tibiae, fibulae, ribs) of 25 specimens (18 identified at the genus level) of different individual sizes and thus possibly ontogenetic stages (Table 2).

The specimen BP/1/5282 identified as *Pareiasaurus* sp., constitutes a rather gracile femur and could correspond to a juvenile specimen of this genus (Fig. 2A,B). The specimen SAM-PK-1058 (described by Lee, 1997a), also called Welgevonden pareiasaur, is of a moderate size (with a snout-vent length of 1.6 m) and according to Lee (1997a) presents atypical features that are absent in all other pareiasaurs. This specimen could constitute a new species of pareiasaur (Lee, 1997a). The sampled specimen of *Pareiasuchus nasicornis* (SAM-PK-K6607) has been described as a juvenile by Lee et al. (1997).

Thin-Section Preparation and Histological Descriptions

Considering that it is sometimes technically challenging to obtain complete thin-sections from large specimens, a method of core drilling was adopted in most cases (Table 2, Fig. 2). This method, inspired from the technique described in Stein and Sander (2009) and already used for paleohistological studies (e.g., Scheyer and Sander, 2007; Redelstorff and Sander, 2009; Redelstorff et al., 2013), leads to the least possible damage to the overall anatomy of skeletal elements. Unlike the standard coring method using a core drill (Stein and Sander, 2009), we utilized high-pressure waterjet cutting technology to core our samples (at CHANTEX heavy Mach., Cape Town, South Africa). This coring methodology allows more flexibility in terms of selection of the size and the shape of the bone cores (i.e., cores are not restricted to the circular and standardized drill bits), and takes on average 5 min to obtain a core sample (as opposed to an hour for the standard core drilling technique developed by Stein and Sander, 2009). We sampled square bone cores (1 × 1 cm) at the midshaft of limb bones (Fig. 2B,F). When possible, the sampling location was away from crests, flanges and areas of strong muscle attachment (i.e., the postaxial flange of the femur of most pareiasaurs, Fig. 2F), which are usually more remodeled than other parts of the cortex or can show unusual growth features (Francillon-Vieillot et al., 1990; Chinsamy-Turan, 2012; Padian and Lamm, 2013). A single femur was completely cut transversally at the midshaft level (specimen BP/I/5282; Fig. 2C–F). A cast of this bone was prepared before thin sectioning. The shape of its cross-section is representative of the overall shape found in most other pareiasaur femora with more or less developed post-axial flange and internal trochanter. Femoral core samples were taken from the dorsal side to the ventral side between the post-axial flange and the internal trochanter (Fig. 2).

Thin-sectioning was conducted at the University of Cape Town, Department of Biological Sciences, using the technical procedures of Chinsamy and Raath (1992) and Padian and Lamm (2013). The histological descriptions follow the terminology used in Francillon-Vieillot et al. (1990) and Chinsamy-Turan (2005).

RESULTS

The degree of bone microstructure preservation is quite variable among the pareiasaurs studied, sometimes even with different preservation in skeletal elements from the same individual. In general, the large and more basal forms, such as *Bradysaurus*, from the *Tapinocephalus* and *Pristerognathus* AZs present poorly preserved bone histology, with the exception of some specimens (e.g., specimen SAM-PK-9355). In most specimens from these AZs, the bone degradation affects both the microanatomical and histological levels. In some sections, the outermost layer of the bone is missing probably due to bone weathering. Moreover, most of the bones sampled present micro-cracks or larger fractures in the cortex. Sometimes the amount of cracks is so extensive that most of the bone microstructure is altered. In some skeletal elements, the medullary cavity is infilled by infiltrating minerals, and in several elements the original birefringence of the bone tissue has been lost. The extensive diagenetic alteration of some skeletal elements limits our histological descriptions and thus the paleobiological interpretations.

The overall bone microstructure tends to be better preserved in the geologically younger genera *Pareiasaurus*, *Pareiasuchus*, and *Anthodon* from the *Tropidostoma* to *Dicynodon* AZs.

We begin the histological descriptions with the clearly identified large and more basal genera recovered from the *Tapinocephalus* and *Pristerognathus* AZs (Figs. 3–5). Specimens found to be misidentified (designated as Pareiasauria Indet. in Table 2), and all recovered from the *Tapinocephalus* AZ, are treated in a separate paragraph (Figs. 6 and 7). These are followed by the medium-sized to small and more derived pareiasaurs *Pareiasaurus*, *Pareiasuchus*, and *Anthodon* (Figs. 2, 8 and 9).

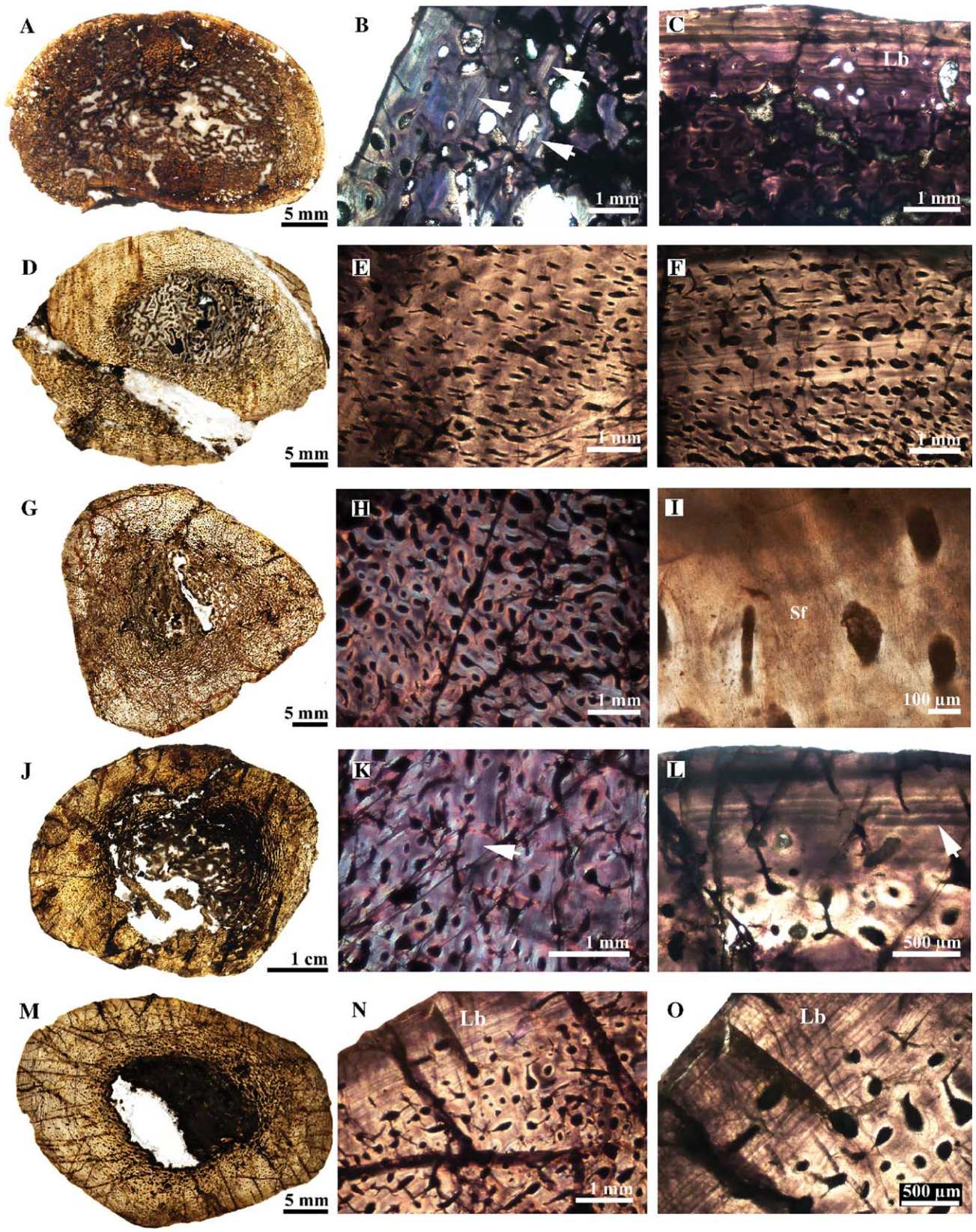
A
5 mm
B
1 mm
C
Lb
1 mm
D
5 mm
E
1 mm
F
1 mm
G
5 mm
H
1 mm
I
Sf
100 µm
J
1 cm
K
1 mm
L
500 µm
M
5 mm
N
Lb
1 mm
O
Lb
500 µm

Fig. 4.

Bone Microstructure of Specimens Identified as *Bradysaurus*

Bradysaurus seeleyi (SAM-PK-9137, femoral length 33.9 cm; SAM-PK-9165, femoral length 40.5 cm). Two different-sized specimens of the most basal pareiasaur species have been sampled.

Three long bones, namely a femur, a tibia and a fibula have been sampled from the smallest individual (SAM-PK-9137; Fig. 3). Between these three bones, the preservation is identical and the diagenetic minerals contained in the bone voids are similar.

The femur and the tibia present a very similar bone microstructure and a rather poor preservation of the bone histology (Fig. 3A–G). The medullary region is infilled with a loose spongiosa (Fig. 3A,D). Nevertheless, only fragments of partly remodeled bone trabeculae remain in the medullary region that is filled with diagenetic mineral cements. The transition between the medullary cavity and the cortical bone is progressive due to intense remodeling in the perimedullary region and the deep cortex. In the deep cortex, the bone remodeling is clearly imbalanced towards resorption, giving the cross-section an overall spongious aspect. The deep bone struts are almost completely remodeled (Fig. 3C). Few remnants of longitudinal primary osteons are visible in the core of these trabeculae, as well as islands of primary parallel-fibered bone (it is difficult to describe the nature of the primary bone matrix, but the preserved osteocyte lacunae are rather round and the matrix is poorly anisotropic). In both elements, the dorsal side of the cortex is thicker and more compact (because of more bone reconstruction) than the ventral side, in which resorption processes seem to be preponderant (Fig. 3A,D). On the dorsal side, the mid-cortex is more compacted with Haversian bone and several generations of secondary osteons (Fig. 3E,F). Most of the secondary osteons preserve a large lumen. Toward the outer cortex, bone remodeling decreases and islands of non-remodeled primary bone are visible between the secondary osteons and resorption spaces (Fig. 3G). The outermost cortex becomes almost avascular and composed of parallel-fibered bone tissue (thicker on the dorsal side of the section and thicker in the femur than the tibia) interrupted by faint growth marks (Fig. 3B). This suggests that the growth of this individual was relatively slow prior to death. Numerous Sharpey's fibers are visible in the outermost cortical layer of the tibia.

The fibula preservation and microstructure are congruent with the above descriptions for the femur and tibia, but some differences are noted (Fig. 4A–C). The medullary cavity is infilled by a dense network of bone trabeculae and the voids are occupied by mineral diagenetic cements. The remodeling is intense in the deep and mid-cortex forming thick trabeculae, such that the transition between the medullary region and the cortex is not well defined. Some large (sometimes cross-cutting) secondary osteons, as well some erosion spaces are visible in the mid-cortex (Fig. 4B,C). Towards the periphery, bone remodeling and vascularization decrease and a primary lamellar-zonal bone [i.e., in this case, a parallel-fibered bone, interrupted by several lines of arrested growth (LAGs)] is visible (Fig. 4B). The spacing between the LAGs decreases between the mid-cortex and the outermost layer. The outer cortex (when preserved) is composed of a poorly vascularized lamellar bone interrupted by closely spaced LAGs (Fig. 4C). The histology of the fibula confirms that the individual was growing slowly at the time of death.

From specimen SAM-PK-9165, a larger left femur was sampled. Here too, the bone histology is poorly preserved but it is evident that it differs in some ways from the smaller individual SAM-PK-9137 described above (Fig. 3H–J). The medullary cavity is infilled by slender and broken bone trabeculae (the rest is infilled by diagenetic mineral cements) and the transition between the medulla and the cortex is progressive. Remodeling is intense in most of the cortex, but clearly imbalanced towards resorption at this stage, resulting in large erosion spaces with very limited subsequent bone redeposition (Fig. 3H–J). It gives a cancellous aspect to the overall bone. More primary bone remains visible in the deep and mid-cortex than in the smaller specimen SAM-PK-9137. The primary bone tissue is a well-organized parallel-fibered tissue in the deeper cortex and turns progressively into a more lamellar bone towards the periphery. Some LAGs interrupting the parallel-fibered bone matrix are visible (Fig. 3J) in the mid-cortex (because bone remodeling was less intense than in the other specimen SAM-PK-9137). The osteocyte lacunae are numerous, dense and small and relatively well organized (Fig. 3J). Few, small primary osteons are still visible in the primary bone matrix in the mid and outer cortex (Fig. 3I). Towards the

Fig. 4. Bone microstructure of the large pareiasaur specimens identified as *Bradysaurus* (**A–I**) and *Embrithosaurus* (**J–O**). A: Diaphyseal cross-section of a fibula of specimen SAM-PK-9137 (maximal diameter: 35.5 mm). B: Detail of the outer cortex of the fibula in A. The primary bone is lamellar-zonal. Note the growth marks indicated by the arrows. C: Detail of the outer cortex of the fibula in A. D: Diaphyseal cross-section of the right fibula of specimen SAM-PK-5127 (maximal diameter: 41.8 mm). E: Detail of the inner cortex of the fibula in D. The cortex is highly vascularized and formed of a lamellar-zonal bone tissue. The orientation and density of the vascular canals vary within the section. The vascularization mostly consists of enlarged primary osteons and incipient secondary osteons. Note the change in vascularization in the inner cortex. F: Detail of the mid-cortex in the fibula in D. A clear annulus of less vascularized lamellar bone is visible. G: Diaphyseal cross-section of the left fibula of specimen SAM-PK-5127 (maximal diameter: 38.97 mm). H: Detail of the inner cortex of the fibula in G. The inner cortex contains numerous secondary osteons with a large lumen. I: Close up on the primary bone in the fibula in D. Sharpey's fibers, oriented parallel to the neighboring vascular canals, are visible throughout the compact cortex. J: Diaphyseal cross-section of the radius of specimen SAM-PK-9128 (maximal diameter: 48.09 mm). K: Detail of the inner cortex of the radius in J. The primary bone is composed of well-vascularized lamellar-zonal bone. Note the growth mark in the inner cortex (arrow). L: Detail of the outer cortex of the radius in J. Note the four LAGs indicated by the arrow. M: Diaphyseal cross-section of the fibula of specimen SAM-PK-9128 (maximal diameter: 36 mm). Note that despite the poor preservation of the medullary region, evidences show that bone trabeculae were present. N, O: Details of the outer cortex of the fibula in M. In the outer cortex, a thick layer of poorly vascularized lamellar bone, interrupted by closely spaced LAGs, represent a slow down of the growth. Abbreviations: Lb, lamellar bone; Sf, Sharpey's fibers.

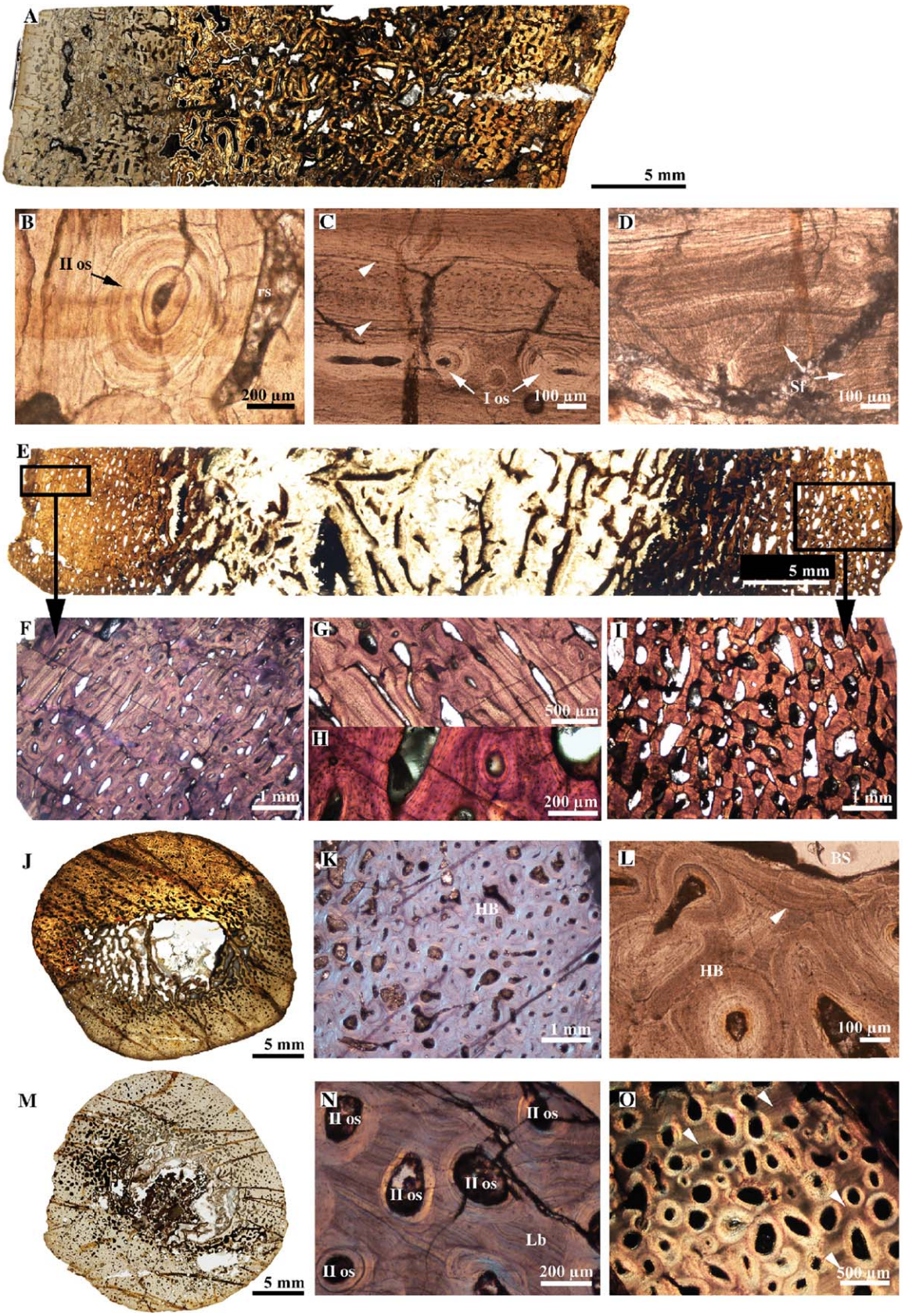
A
5 mm
B
II os
FS
200 µm
C
I os
100 µm
D
Sf
100 µm
E
5 mm
F
1 mm
G
500 µm
H
200 µm
I
1 mm
J
5 mm
K
HB
1 mm
L
BS
HB
100 µm
M
5 mm
N
II os
II os
II os
II os
Lb
II os
200 µm
O
500 µm

Fig. 5.

periphery, bone remodeling and vascularization decrease. Few primary osteons and some radial canals are visible in the outer cortex (Fig. 3I). Once again, the compact cortex of the dorsal side of the bone is thicker than the ventral side and shows a thicker layer of poorly vascularized parallel-fibered to lamellar bone with several, but faded LAGs in the outer cortex. The spacing between the LAGs does not seem to decrease drastically in the periphery of the bone (Fig. 3I). This individual was still growing (although slowly) at the time of death.

Bradysaurus baini *(SAM-PK-5127, femur length 45 cm; SAM-PK-3533)*

Two different specimens associated with this basal pareiasaur species have been sampled. For specimen SAM-PK-5127, which is the largest individual in our sample, we initially sampled three elements (one femur and two fibulae). However, the preservation of the femur histology is too poor to be described in detail here. We can nonetheless note that the overall bone microstructure is similar to the femur of *B. seeleyi* SAM-PK-9137.

In the first fibula, the medullary cavity is almost completely occupied by bone trabeculae (Fig. 4D). The voids in the medullary region show diagenetic recrystallization. The perimedullary region is remodeled. Most of the cortex is formed of a highly vascularized lamellar-zonal bone (the matrix is parallel-fibered to lamellar) with numerous, enlarged primary and some incipient secondary osteons. The incipient secondary osteons do not crosscut each other but they do intersect the growth marks (Fig. 4F). The orientation of the vascular canals is variable within the section (Fig. 4E,F). In the mid-cortex, a distinct layer of poorly vascularized lamellar bone is likely a broad annulus, suggesting a prolonged period of slower growth (Fig. 4F). There are bundles of Sharpey's fibers in the bone matrix throughout the cortex and these fibers seems to be oriented parallel to the vascular canals (Fig. 4I). In the bone periphery, the bone vascularization decreases and several clear LAGs are visible.

The second fibula (Fig. 4G) presents a similar bone microstructure, although the Haversian substitution is more advanced such that the amount of primary bone tissue preserved in the cortex is lower than in fibula 1. Also, the transition between the medullary cavity and the compact cortex is much more gradual than in the other fibula because the resorption is more pronounced in the perimedullary region. The pattern of bone remodeling is variable within the section. Some regions are rather spongious almost up to the bone surface; others are more compact with patches of Haversian bone (the secondary osteons nonetheless preserve a large lumen; Fig. 4H). Finally, as for the other fibula, the pattern of vascular orientation differs greatly within the section. Some avascular and non-remodeled primary lamellar bone with closely spaced rest lines is visible in the outermost cortex (where the bone surface is preserved).

Two ribs have been sampled from specimen SAM-PK-3533 (Fig. 5J–O). In both elements, the cortex is thick and rather compact. The medullary region is well delimited with few bone trabeculae. The bone remodeling is asymmetrical in both elements. In diametrically opposed areas of the section, the cortex is highly remodeled up to the surface and formed of dense Haversian bone with several generations of cross-cutting secondary osteons (Fig. 5K,L). The remodeling is extensive and sometimes even the bone surface has been remodeled, as evidenced by the presence of scalloped cementing lines (Fig. 5L). Other regions of the bone are less remodeled and the primary bone is still visible and formed of a lamellar-zonal bone matrix with scattered secondary osteons (Fig. 5N,O). These secondary osteons can have variable sizes and shapes (Fig. 5K,L,N,O), but have a preferential longitudinal orientation. Numerous drifting osteons are present in the ribs. In some regions of the outermost cortex, a layer of unremodeled and avascular lamellar bone with closely spaced rest lines is visible.

Bradysaurus *sp.* *(SAM-PK-12057, femur length 22.2 cm; SAM-PK-12129, femur length 24.2 cm; SAM-PK-9355, femur length 28.6 cm; SAM-PK-12047; BP/I/5430)*

Most of these specimens have a similar bone histology to that of the *B. seeleyi* specimens described above and are therefore not all described separately in detail.

However, since SAM-PK-12057 represents the smallest specimen identified as *Bradysaurus* in our sample, the histology of its femur and tibia are described in more detail here (Fig. 5A–D). Both skeletal elements have been strongly altered by diagenesis. The medullary cavity is completely infilled by a dense network of bone trabeculae, and the inner cortex is highly remodeled such that the transition between the compact cortex and the medullary region is ill defined and the cross-sections have an overall spongious aspect (Fig. 5A). The remodeling, and especially bone resorption seems to be stronger on the ventral side than the dorsal side, giving the latter a more compact texture (Fig. 5A). The vascularization and secondary reconstruction decrease towards the periphery of the bone (Fig. 5A) suggesting a slowing

Fig. 5. Bone microstructure of large pareiasaur specimens identified as *Bradysaurus*. **A**: Bone core of the tibia of specimen SAM-PK-12057 (length: 33 mm; dorsal side to the left, ventral to the right). **B**: Detail of the outermost cortex of the dorsal side of the tibia in A, with a well-preserved secondary osteon. **C**: Detail of the outermost cortex of the tibia in A. Note the alternation of poorly vascularized layers of lamellar and parallel-fibered bone. The arrowheads point at LAGs. **D**: Detail of the outermost cortex of the tibia in A. Numerous Sharpey's fibers are visible in the primary bone matrix. **E**: Bone core of the femur of specimen SAM-PK-9355 (length: 52 mm; dorsal side to the left and ventral side to the right). **F**: detail of the cortex on the dorsal side of the femur in E. **G–H**: inner cortex (detail from E). **I**: Detail of the cortex on the ventral side of the femur in E. **J**: Cross-section of a rib of specimen SAM-PK-3533 of *Bradysaurus baini* (maximal diameter of the section: 26.4 mm). **K**. Detail of the cortex of the rib in J. Most of the cortex is highly remodeled and formed of dense Haversian bone. **L**: Haversian bone up to the bone surface with several generations of secondary osteons. Even the bone surface has been remodeled in this area as attests a clear reversal line (arrow head) cross-cuting the underlining secondary osteons. **M**: Cross section of another rib of the specimen SAM-PK-3533 (maximal diameter of the section: 23.6 mm). **N**, **O**: The remodeling of the cortical bone is asymmetrical and the Haversian bone is less dense in some regions of the bone than in others. Several growth marks are visible (arrow heads) in the primary lamellar bone. Abbreviations: BS, bone surface; II os, secondary osteons; Lb, Lamellar bone; HB, Haversian bone; Sf, Sharpey's fibers.

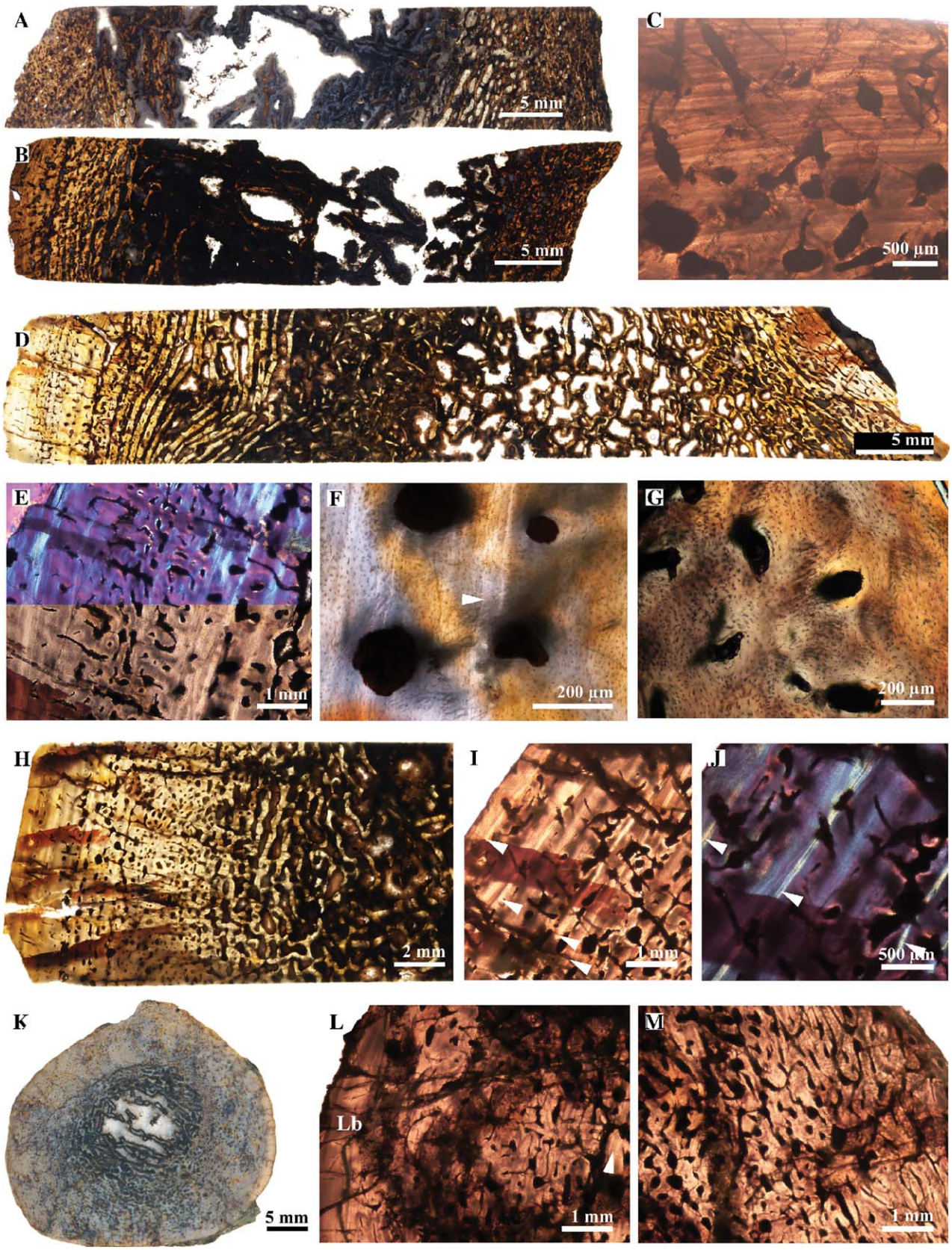
A
5 mm
B
5 mm
C
500 µm
D
5 mm
E
1 mm
F
200 µm
G
200 µm
H
2 mm
I
1 mm
J
500 µm
K
5 mm
L
Lb
1 mm
M
1 mm

Fig. 6.

down in the rate of bone deposition. The outer cortex is formed of poorly vascularized parallel-fibered to lamellar bone (the birefringence and size of the osteocyte lacunae differ between the different layers; Fig. 5C) and the vascular canals are arranged as longitudinal primary and secondary osteons (Fig. 5B,C). LAGs are visible in the outermost cortex, as well as numerous Sharpey's fibers (Fig. 5C,D).

The left femur of specimen SAM-PK-9355 has been sampled. The bone histology is relatively well-preserved, as compared to the other *Bradysaurus* specimens. The overall microanatomy is similar to the femur of specimen SAM-PK-12129 (of similar size). The medullary cavity is infilled by slender bone trabeculae and the transition between the medullary region and the compact cortex is progressive but rather conspicuous (Fig. 5E). A difference in the pattern of remodeling between the ventral (resorption in favour of redeposition) and dorsal side is noticeable, such as the ventral side appears more spongious (even though the trabeculae are almost completely remodeled) and the dorsal side more compact (more redeposition; Fig. 5E-I). On the dorsal side, the mid-cortex has many secondary osteons (Fig. 5F–H). The vascular canals have in general a longitudinal or circumferential organization. On both sides of the section, most of the outermost cortex is missing, probably due to weathering. However, in the preserved portion of outer cortex of the dorsal side, the bone tissue becomes less remodeled and less vascularized suggesting a decrease in the bone depositional rate (Fig. 5F).

Bone Microstructure of Specimens Identified as *Embrithosaurus* (SAM-PK-9128, Femur Length 30.8 cm; SAM-PK-9116)

Two specimens identified as *Embrithosaurus* in the Iziko South African Museum collections (Cape Town, South Africa) were studied histologically. Both of these showed similar bone tissue structures as observed in *Bradysaurus*.

SAM-PK-9116 (not figured). Both a femur and a radius sampled from this medium-sized specimen identified as *Embrithosaurus* sp. showed congruent (though mostly poorly preserved) bone microstructure (and diagenetic alterations in terms of bone coloration, and mineral infiltrations). The medullary region is infilled by thin-bony trabeculae (fairly broken in the femur) and the deep cortex is highly remodeled giving a cancellous aspect to it. Nevertheless, the transition between the cortical region and the medullary cavity remains conspicuous. From the mid-cortex to the periphery of the bone, the remodeling and the vascularization of the bone tissue decrease, giving a more compact aspect to the outermost cortex (at least on the dorsal side for the femur).

SAM-PK-9128. A fibula and a radius have been sampled from this specimen (Fig. 4J–O) and exhibit similar bone tissues and poor preservation with many cracks across the cortex (Fig. 4J,M).

In the fibula (Fig. 4M–O), the overall bone microstructure is very similar to that observed in the fibulae of specimen SAM-PK-5127 *Bradysaurus baini*. The medullary cavity is filled with a loose network of thin bony trabeculae, which were broken post mortem. The cortex is thick and rather compact. In some parts of the section, dense Haversian bone occurs; in other parts, the Haversian substitution is less pronounced and islands of primary lamellar-zonal bone are still visible between isolated secondary osteons (with a large lumen; Fig. 4N,O). The vascularization varies greatly in terms of density and orientation within the section. A thick layer of almost avascular lamellar bone with closely spaced rest lines is present in the outer cortex (suggesting that growth had drastically slowed down at the time of death; Fig. 4N,O).

The bone histology of the radius is similar and congruent with the fibula (Fig. 4J–L), although secondary reconstruction is less extensive, and growth marks are visible in the mid-cortex (Fig. 4K). The peripheral part of the bone wall shows a thin layer of lamellar bone associated with multiple and closely spaced growth marks (Fig. 4L) congruent with a slowing down of growth.

Bone Microstructure of Unidentified Specimens from the *Tapinocephalus* AZ

The bone microstructure of several unidentified pareiasaur elements from the *Tapinocephalus* AZ has been

Fig. 6. Bone microstructure of unidentified pareiasaur specimens from the *Tapinocephalus* assemblage zone. **A**: Bone core of a femur of specimen SAM-PK-4996 (length: 48 mm; dorsal side to the left, ventral side to the right). Both dorsal and ventral outermost layers of the cortex are missing. **B**: Bone core of a femur of specimen SAM-PK-4344 (length: 45.5 mm; dorsal side to the left, ventral side to the right). **C**: Detail of the outer cortex of the dorsal side of the femur in B. Note the decrease in bone remodeling and vascularization in the outer cortex with the slow apposition of lamellar bone. **D**: Bone core of the right femur of specimen SAM-PK-K322 (length: 61 mm; dorsal side to the left, ventral side to the right). **E**: Detail of the outer cortex on the dorsal side of the femur in D in polarized light (top) and direct light (bottom). This outer cortex is made of a poorly remodeled parallel-fibered to lamellar bone matrix. Several growth cycles of variable thickness are identifiable. **F**: Detail of the primary cortical bone with simple vascular canals and primary osteons. The primary bone matrix is constituted of a parallel-fibered to lamellar bone matrix. The osteocytes lacunae are small and numerous. Patches of Sharpey's fibers are scattered in the bone matrix and around the vascular canals. The arrow points to a thin annulus of avascular lamellar bone. **G**: Detail of the external layer of the cortex with simple vascular canals, primary osteons and patches of Sharpey's fibers. Locally, the Sharpey's fibers give to the bone matrix a rather woven aspect since the neighboring osteocyte lacunae have a random organization. **H**: Dorsal side of the bone core of the right tibia of specimen SAM-PK-K322 (length: 17.6 mm; complete bone core length: 41.3 mm). **I**,**J**: Details of the outer cortex of the tibia in H (direct light in I, polarized light in J). Thin annuli associated with clear LAGs (arrow heads) are visible in the outer cortex. The spacing between the LAGs does not seem regular. As in the associated femur, the darker areas in the bone matrix consist of bundles of Sharpey's fibers. **K**: Diaphyseal cross-section of the fibula of specimen SAM-PK-1574 (maximal diameter: 33.2 mm). **L**: Detail of the cortex of the fibula in K. Note the annulus of avascular lamellar bone in the mid-cortex (arrowhead) followed by a zone of the cortex affected by Haversian substitution. The outermost layer is formed of a poorly vascularized lamellar bone. **M**: The vascularization pattern is very variable within the section. Abbreviation: Lb, lamellar bone.

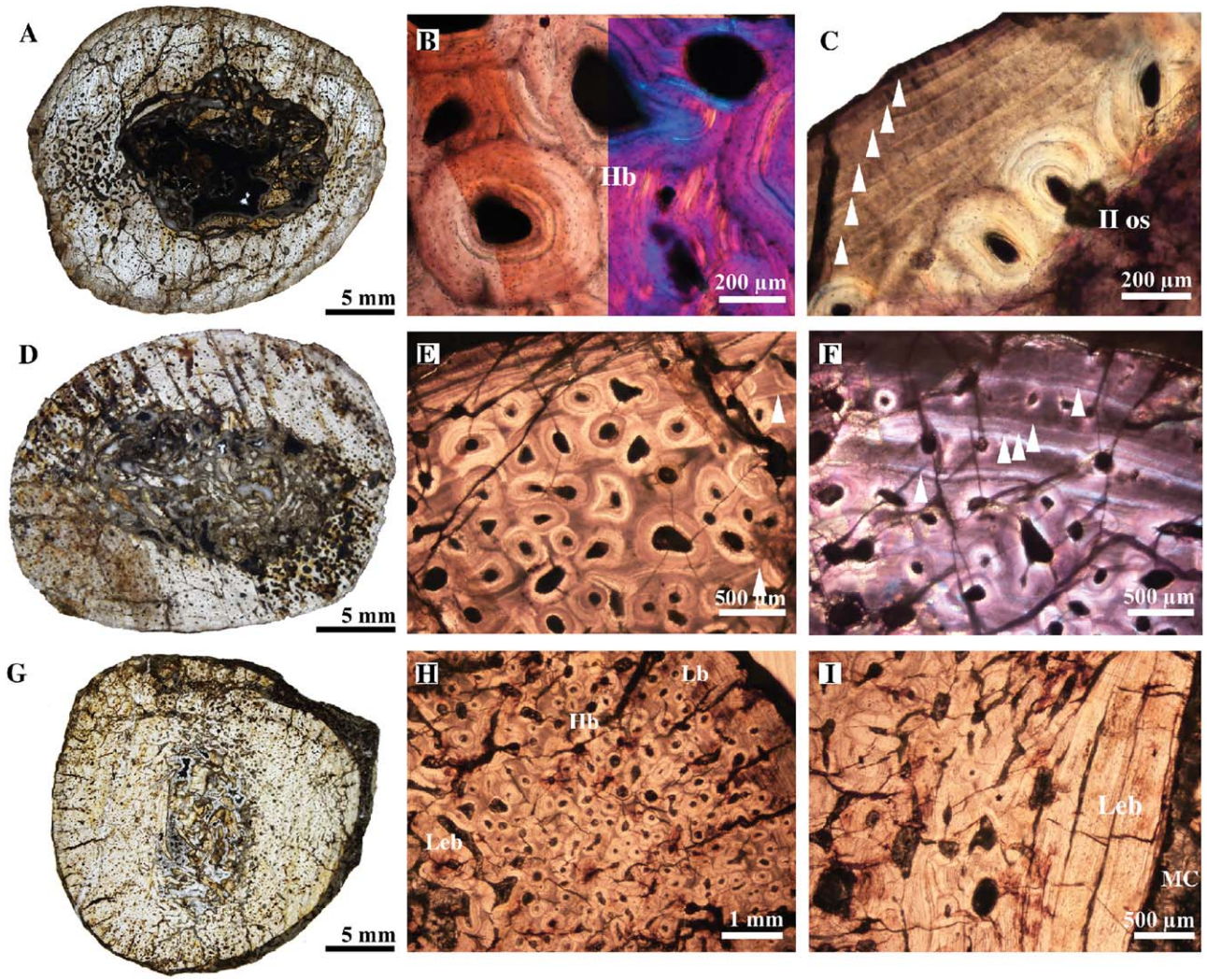

Fig. 7. Bone microstructure of ribs of unidentified pareiasaur specimens from the *Tapinocephalus* Assemblage Zone. **A**: Cross-section of a rib of specimen BP/I/1574 (maximal diameter: 26 mm). **B**: Detail of the cortex of the rib in A. Part of the cortex is formed of a dense Haversian bone with several generation of crosscutting secondary osteons. **C**: Detail of the outermost layer of the cortex of the rib in A, formed of a slowly deposited avascular lamellar bone. Note the record of LAGs (at least 6 visible, arrow heads). **D**: Cross-section of another rib of specimen BP/I/1574 (maximal diameter: 24.6 mm). **E**,**F**: Detail of the cortical bone of the rib in D. Some parts of the mid-cortex are highly remodeled and formed of Haversian bone. Other areas of the section are less affected by Haversian substitution and the primary lamellar bone, interrupted by LAGs (arrow heads), is visible. **G**: Cross-section of a rib of specimen SAM-PK-6554 (maximal diameter: 25.5 mm). **H**: Detail of the cortex organization of the rib in G. The medial side is bordered by endosteal lamellar bone. The deep cortex is mostly formed of dense Haversian bone. The outer cortex is formed of a poorly vascularized lamellar bone. **I**: Detail of the inner cortex and the centripetally deposited lamellar endosteal bone. Abbreviations: Hb, Haversian bone; Lb, lamellar bone; Leb, lamellar endosteal bone; MC, medullary cavity; II os, secondary osteon.

studied. Overall, it resembles the bone microstructure of the pareiasaurs identified as *Bradysaurus* and *Embrithosaurus*. However, it is worth noting that the femur of SAM-PK-4344, although small, appears to show histological evidence of having ceased growth.

SAM-PK-4996. A single femur has been sampled for this small specimen. The bone microstructure is really similar to that of the femora of specimens SAM-PK-10057, 12129, and 9355 (Fig. 6A). However, the outermost cortex is missing on the dorsal and ventral side of the bone core.

SAM-PK-4344. The right femur has been sampled on this small specimen (Fig. 6B). The bone histology is poorly preserved and cracks are covering the complete bone core. The cortex seems thicker on the dorsal side than on the ventral side, but part of the bone surface seems to be missing on the ventral side. On the dorsal side, the deep cortex is highly remodeled and has a spongious aspect. Some islands of primary bone remain in the mid-cortex between resorption cavities and incipient secondary osteons and consist of a lamellar-zonal bone (Fig. 6C). The spacing between the LAGs decreases from the mid-cortex to the outermost cortex, along with bone vascularization and remodeling. A thick layer of

lamellar bone with closely spaced rest lines is visible in the outercortex (Fig. 6C). The specimen was probably already mature at the time of death.

SAM-PK-K322. A femur and a tibia have been sampled for this specimen (Fig. 6D,H). The bone microstructure is well preserved and similar in both skeletal elements (Fig. 6D–J). The medullary cavity is infilled by a dense network of bone trabeculae (Fig. 6D). Once again, the dorsal side of the bone is thicker and more compact than the ventral side in both elements. The deep cortex is highly remodeled with an imbalance towards resorption, resulting in a spongious texture. On the dorsal side of the femur, the bone trabeculae of the deep cortex have a regular and preferential circumferential organization (as observed also in the femur of other individuals; Fig. 6D). In both elements, the external half of the cortex is less remodeled and mostly composed of primary bone tissue (Fig. 6E–G,I,J). The vascularization is mostly formed of simple vascular canals and primary osteons (Fig. 6E–G,I,J). The vascular canals are preferentially longitudinal, but with many anastomoses for example in the highly vascularized zone in the femur (Fig. 6E). Some of these primary osteons also seem to be partly eroded (Fig. 6E,I,J). Secondary reconstruction is more advanced in the deep cortex of the tibia with more redeposition giving some isolated incipient secondary osteons. In both elements, the cortex shows some cyclicality in the deposition of bone (lamellar-zonal bone) with an alternation of well-vascularized zones with a parallel-fibered bone matrix, and narrower, poorly vascularized to avascular, lamellar or parallel-fibered annuli (Fig. 6I,J) that sometimes present clear LAGs (Fig. 6I,J). Sharpey's fibers are abundant around the vascular canals in the parallel-fibered bone (Fig. 6F,G). In general, the osteocyte lacunae are abundant and rather well organized throughout the cortex. However, in the vicinity of Sharpey's fibers they tend to be disorganized and appear rather round (as in woven bone). In both skeletal elements, the cortex seems to become less vascularized toward the periphery. However, the cyclicality is not regular and the width of the zones and annuli seems to be variable. It is thus difficult to estimate whether or not bone growth had already slowed down in this individual.

Fibulae of specimens BP/I/1574 and SAM-PK-8948. The microstructure of the fibula BP/I/1574 is similar to that observed in other specimens identified as *Bradysaurus* and also shows variability in the pattern of vascularization within the section (Fig. 6L,M).

In both elements the preservation of the bone structure is poor. The cortex is thick and the medullary cavity is infilled by few bony trabeculae. The perimedullary region is remodeled such that the transition between the cortex and the medullary cavity is not well defined. The remnants of non-remodeled primary cortex attest to a lamellar-zonal bone. Lots of Sharpey's fibers are visible in the primary bone matrix of fibula SAM-PK-8948. The fibula of BP/I/1574 has a thick and rather compact cortex (Fig. 6K–M). Some zones in the deep cortex are highly remodeled with numerous secondary osteons. Narrow annuli of lamellar bone are still visible in the non-remodeled parts of the deep cortex (Fig. 6L). The outermost cortex is formed of a thick layer of poorly vascularized lamellar bone (Fig. 6L).

Ribs of BP/I/347, BPI/I/1574, SAM-PK-3353, SAM-PK-6554. Overall, the ribs have a similar bone microstructure with a variable degree of preservation and Haversian substitution (Fig. 7). The cortex is compact and thick. The medullary cavity is more or less infilled by bony trabeculae. Most of the rib cross-sections present a heterogeneous distribution of Haversian bone. In some localized regions of the sections, the deep cortex is highly remodeled, but the remodeling is in favor of the resorption process (Fig. 7A,D,G). In these regions, the deep cortex has a cancellous aspect and the primary cortical bone matrix is still visible. The primary bone is formed of lamellar-zonal tissue with some scattered longitudinal primary, but mostly secondary osteons (Fig. 7E,F). The secondary osteons preserve a large Haversian canal. In some ribs, the outermost cortex is less remodeled and formed of a layer of avascular lamellar bone with closely spaced LAGs (Fig. 7C,H). In other regions, the Haversian substitution is more intense and the cortex is composed of dense Haversian bone with several generations of secondary osteons, sometimes almost up to the bone surface (Fig. 7B,H). In some ribs, the medullary region is bordered by a thick layer of endosteally formed lamellar bone (Fig. 7I).

Bone Microstructure of *Pareiasaurus* sp. (BP/I/5282, Femur Length 22 cm; SAM-PK-10032, Femur Length 32 cm)

BP/I/5282. This is a small specimen identified as *Pareiasaurus* sp. The complete mid-diaphyseal cross-section of the femur is the only one we were able to obtain, and it is representative of the overall shape found in most other pareiasaur femora (Fig. 2F). The medullary cavity is infilled by secondary bone trabeculae and the section of the bone is mostly spongious in appearance since the preserved compact cortex is thin (the thickness of the compact cortex is variable around the section, but is higher on the dorsal side than on the ventral side of the bone, as observed in other pareiasaur femora; Fig. 2C–F). Most of the cortex has been remodeled with an imbalance towards resorption (Fig. 2F–H). By this process, the deepest part of the primary cortex is progressively changed into a spongiosa formed mostly of secondary lamellar bone (Fig. 2F,J). The mid-cortex is also highly remodeled and present large erosion cavities with thin lining of endosteal lamellar bone, as well as large incipient secondary osteons (Fig. 2G–I). Despite an extensive bone remodeling, patches of primary bone are still visible in the mid-cortex and consist of a relatively well-vascularized lamellar-zonal bone (parallel-fibered bone matrix) with small longitudinal primary osteons (Fig. 2G,I). Each zone seems to have contained one or several layers of primary osteons. The annuli are thin, formed of avascular lamellar bone and contain usually one LAG (Fig. 2H). In the outer cortex, the bone organization changes with the deposition of a poorly vascularized and rather thick layer of lamellar bone interrupted by several rest lines. No primary osteons are visible in this layer; however it contains few simple radial canals (Fig. 2G,H). This sudden change in bone deposition rate suggests that after a period of relatively faster growth,

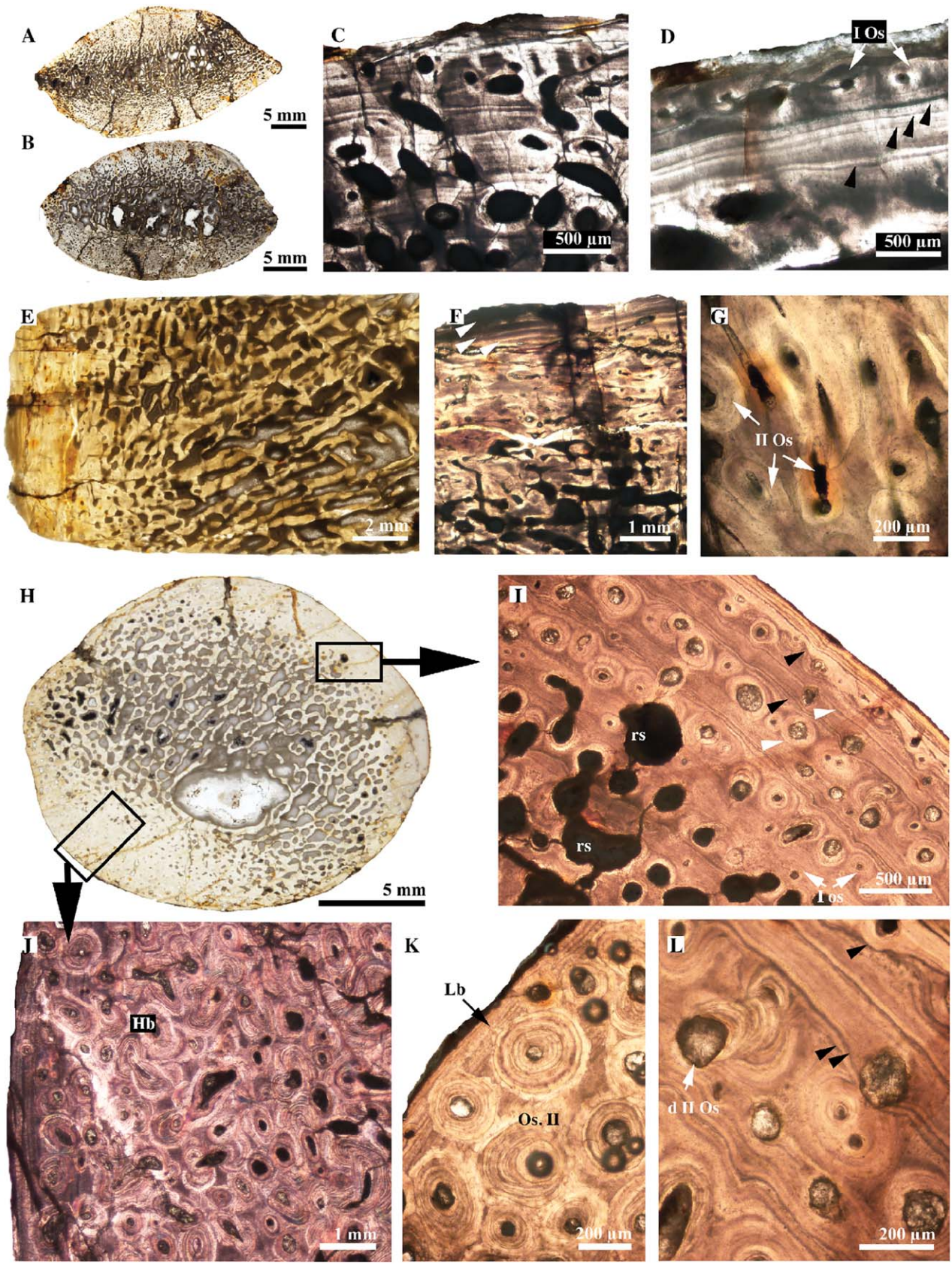
A
5 mm
B
5 mm
C
500 µm
D
I Os
500 µm
E
2 mm
F
1 mm
G
II Os
200 µm
H
5 mm
I
rs
rs
I Os
500 µm
J
Hb
1 mm
K
Lb
Os. II
200 µm
L
d II Os
200 µm

Fig. 8.

the growth of the individual slowed down significantly. From the few areas of primary bone preserved in the mid and outer cortex, it is evident that there was a faster growth during early ontogeny (with more widely spaced growth marks), followed by a reduction in the spacing of the LAGs together with a decrease of vascularization and remodeling (Fig. 2H). Finally, throughout the section, the osteocyte lacunae are small but abundant.

SAM-PK-10032 (not figured). A femur and a tibia have been sampled for this specimen. The bone microanatomy is similar to that of the femora and tibia of specimens SAM-PK-12057, 12129, 9355, and 9137. The histological preservation is poor and the outermost cortex is missing probably due to the weathering of the bone surface. The mid-cortex seems to be formed by a dense Haversian bone tissue.

Bone Microstructure of the Welgevonden Pareiasaur (SAM-PK-1058)

The histology of the humerus is poorly preserved and the outermost cortex is missing. However, it seems that the cortex preserved a rather compact aspect. The medullary cavity is completely infilled by bone trabeculae (rather dense network). The deep cortex is quite spongious. Part of the mid-cortex is preserved and seems to be highly remodeled, as suggests the presence of numerous large secondary osteons (with a large lumen). Because of the poor preservation, no growth-cycle can be observed.

The ribs cross-sections have a rather fusiform shape (Fig. 8A,B), unlike the ribs of sampled pareiasaurs from the *Tapinocephalus* AZ. Within a rib cross-section, the extent of bone remodeling varies greatly. The extent of Haversian substitution also differs between the elements and the level of the section. In the different elements, the medullary cavity is infilled by bone trabeculae and the deep cortex is highly remodeled such that the transition between the medullary region and the cortical region is rather progressive. Haversian substitution is more or less extensive in the cortex. In some parts of the cortex, Haversian substitution is extensive and reaches the bone surface, with several generations of secondary osteons. In other regions, the primary bone tissue is still visible and consists of a poorly vascularized lamellar-zonal bone with sparse and small longitudinal primary osteons and some scattered secondary osteons with large Haversian canals (Fig. 8C,D). Several LAGs are visible throughout the cortex in the regions where the bone remodeling is less intense (Fig. 8C,D). These LAGs appear sometimes in groups of 2 to 4 consecutive and closely spaced lines (Fig. 8D).

Bone Microstructure of *Pareiasuchus nasicornis* (SAM-PK-K6607)

A tibia and a rib from the specimen SAM-PK-K6607 have been sampled. In the tibia, the medullary cavity is infilled by thick bone trabeculae, which form a well-organized mesh (the unusual orientation of the bone trabeculae may be a consequence of the slightly oblique nature of the section; Fig. 8E). Bone remodeling, and particularly bone resorption, are extensive in the deep cortex giving a spongious aspect to the section. Toward the periphery, the bone becomes compacted with well-developed secondary osteons (Fig. 8F,G). Even though part of the outermost cortex is missing, it is noticeable that bone vascularization decreases drastically close to the periosteal surface and a layer of lamellar bone with closely spaced rest lines is present (Fig. 8F).

The rib presents a good histological preservation with a thick cortex and a small medullary cavity, free of bone trabeculae and partly bordered by a layer of endosteal lamellar bone (Fig. 8H). As in almost all other pareiasaurian ribs, the pattern of bone remodeling is asymmetrical. Two opposite regions of the cortex are rather spongious with high remodeling in favor of resorption almost up to the bone surface. As a result, the compact cortex is very thin in these regions. In other parts of the section, bone resorption is less intense and the compact cortex thicker. Haversian substitution can be extreme with several generations of crosscutting secondary osteons (Fig. 8J,K); or limited and part of the initial primary lamellar-zonal bone is visible (Fig. 8I,L). A certain cyclicality in bone deposition is visible in the poorly remodeled cortical regions: a layer of almost avascular lamellar bone (comprising few small primary osteons), which does not encounter much remodeling, is followed by a layer with a single row of secondary osteons (but sometimes several generations, including also drifting osteons). Some secondary osteons preserve a large lumen; others are more mature and show a thick layer of centripetally deposited lamellar bone and a narrow lumen. These two layers seem to be separated by a faint rest line (Fig. 8I,L). In several occasions, directly above the layer with the row of secondary osteons, there is an

Fig. 8. Bone microstructure of medium-sized pareiasaurs from the Upper Permian. The Welgevonden pareiasaur, SAM-PK-10058 (**A–D**) and *Pareiasuchus nasicornis*, SAM-PK-K6607 (**E–L**). A, B: Cross-sections of two ribs [maximal diameter: 35.1 mm (A) and 27.3 mm (B)]. C: Detail of the cortex of the rib in A. The cortex is formed of lamellar-zonal bone. Note the several growth marks in the lamellar bone matrix. D: Detail of the outer cortex of the rib in A. An avascular layer with several closely spaced LAGs (black arrow heads) is followed by a row of small and longitudinal primary osteons. **E**: Bone core of a tibia of *Pareiasuchus* (ventral side—complete bone core length: 42 mm). **F**: Detail of the outer cortex on the ventral side of the tibia in E. The mid-cortex presents a high degree of Haversian substitution. The outermost layer consists of avascular lamellar bone with several closely spaced LAGs (arrow heads). **G**: Detail of the mid-cortex of E. **H**: Cross-section of a rib (maximal diameter: 19.5 mm). The bone remodeling is asymmetrical in the section. **I**: Detail of the outer cortex of the rib in H. The primary bone is lamellar-zonal. The vascularization is organized in concentric layers. The vascular canals are longitudinal. Some faint rest lines (white arrow heads) as well as cement lines (black arrow heads) are visible in this area of the cortex. **J**: Detail of the cortex of the rib in H. Note the dense Haversian bone in this area, up to the bone surface. **K**: Detail of the secondary osteons in the outer cortex in H. **L**: Close up of the cortical bone in I. Some cement lines, corresponding to several erosion episodes of the bone surface, cut the underlying osteons (black arrow heads). Several drifting osteons are visible in the cortex as pointed out here. Abbreviations: I Os, primary osteons; II Os, secondary osteons; d II Os, drifting secondary osteon; Hb, Haversian bone; Lb, lamellar bone; rs, resorption spaces.

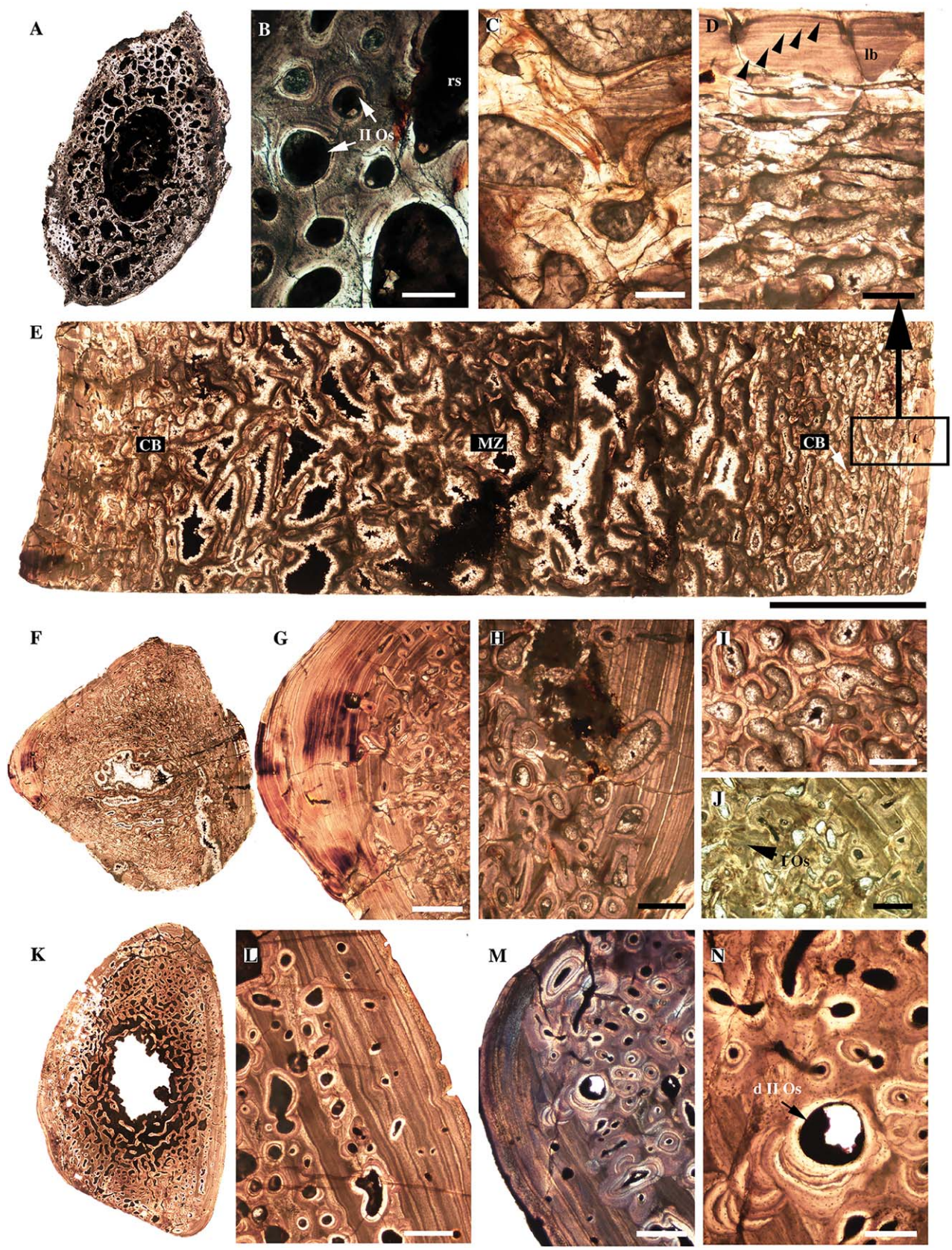

Fig. 9.

irregular structure that seems at first glance to be composed of several closely spaced LAGs. After closer examination, the lines seem to be resorption lines (scalloped lines cross-cutting underlying preexistent structures) representing successive episodes of erosion/reconstruction of the bone surface (Fig. 8L). Finally, even though most of the growth record is not preserved because of extensive cortical remodeling, the spacing between the few growth marks visible in the outer cortex seems to decrease toward the periphery of the bone. Moreover, a thin layer of avascular lamellar bone with closely spaced rest lines is visible in the outer cortex all around the section. These features suggest that growth had already slowed down at the time the animal died.

Bone Microstructure of *Anthodon serrarius*

BP/I/548. A rib fragment from this small specimen has been sampled. The cross-section is incomplete and has part of the outermost cortex missing. However, it is possible to tell that the overall section was not compact because: (i) contrary to other ribs sectioned, the medullary cavity is large, clearly defined, with only few bone trabeculae (Fig. 9D); (ii) the perimedullary region and parts of the mid-cortex are highly remodeled with large erosion cavities (sometimes lined up with a thin layer of lamellar endosteal bone) or large incipient secondary osteons, giving to the section a spongious aspect (Fig. 9A,B). The compact cortex contains numerous incipient longitudinal secondary osteons. These secondary osteons have overall wide Haversian canals (but the diameter of the secondary osteons seems to decrease toward the bone surface). In general, these secondary osteons present a very thin lining of endosteal lamellar bone and can thus be considered as incipient. In some regions of the section, some small primary osteons are also visible. A large amount of primary bone remains but it is very difficult to assess the nature of its matrix because of poor preservation (no osteocyte lacunae visible, no growth marks observable and the bone matrix type is not identifiable). Overall, the rib seems to belong to a young individual (from the diameter which is smaller than the other rib, but also from the degree of Haversian substitution, which is less advanced as compared to the rib of *Anthodon* SAM-PK-10026, and the ribs of other pareiasaurs).

SAM-PK-10074. A femur and a fibula of that specimen, described in Boonstra (1932), have been sampled for thin sectioning. They both present the same preservation state with important recrystallization in the bone voids (Fig. 9E,F). The femur midshaft presents a spongious aspect (Fig. 9E). The medullary region is infilled by a well-developed spongiosa. The inner cortex has been completely remodeled by erosion and reconstruction resulting in a cancellous secondary spongiosa (Fig. 9C,D). The primary bone tissue is no longer visible in the mid and deep cortex. The compact cortex is very thin on both the ventral and the dorsal sides. Towards the periphery, the cortex becomes progressively more compact and few secondary osteons are visible. A thin layer of compact, poorly vascularized lamellar bone with several LAGs (five visible) can be observed in the outermost cortex on both sides (Fig. 9D). The spacing between these LAGs decreases towards the bone surface suggesting that the bone deposition rate slowed down significantly.

The microstructure of the fibula is slightly different. The midshaft presents a small but distinct medullary cavity, free of bone trabeculae (Fig. 9F). The deep cortex has been highly remodeled, with an imbalance toward resorption, resulting in a cancellous aspect of the bone (Fig. 9F,I). In the perimedullary region, the spongiosa is formed by secondary bone trabeculae (Fig. 9I). The mid-cortex is formed by a dense Haversian bone with several generations of secondary osteons (Fig. 9G,H). These secondary osteons have different sizes and orientations, and some of them retain a wide Haversian canal (Fig. 9G,H). Toward the periphery, in some regions of the bone, the remodeling is less intense and remnants of primary lamellar-zonal bone are visible between the secondary osteons. In these regions, the primary bone is lamellar with small and longitudinal primary osteons (Fig. 9H,J). The outer cortex consists of a thick layer of avascular lamellar bone tissue with closely spaced LAGs suggesting a drastic slow down of the growth. A well-preserved growth record (at least 17 or 18 incremental rest lines; and considering that the older growth cycles were destroyed by remodeling processes; Fig. 9G) confirms that this small specimen was not a juvenile. There is a clear decrease in LAG spacing between the first visible ones in the mid-cortex and the more regularly and closely spaced LAGs in the outer lamellar cortex (Fig. 9G).

SAM-PK-10026. A fragment of rib has been sampled from this specimen (Fig. 9K). The bone histology is

Fig. 9. Bone microstructure of the small-sized pareiasaur *Anthodon serrarius*. **A**: Cross section of a rib of specimen BP/I/548 (maximal diameter: 16 mm). **B**: Details of the bone wall of the rib in A. **C**: Secondary bone trabeculae in the deep cortex of the dorsal side of the femur of specimen SAM-PK-10074 in E. **D**: Close up of the outer cortex on the dorsal side of the femur in E. Most of the cortex is spongious. Only a thin layer of compact lamellar bone with closely spaced LAGs (black arrowheads) is visible in the outermost cortex. **E**: Bone core of the femur of specimen SAM-PK-10074 (approximate maximal length: 31 mm; dorsal side to the left, ventral side to the right). **F**: Mid-diaphyseal cross-section of a fibula of specimen SAM-PK-10074 (maximal diameter: 19.7 mm). **G**: Detail of the cortex of the fibula in F. The mid-cortical region is highly remodeled with several generations of secondary osteons. The outer layer is formed of a poorly vascularized lamellar bone interrupted by several closely spaced LAGs. **H**: Close up of the transition between the heavily remodeled cortex and the avascular lamellar bone deposit. **I**: Detail of the spongiosa in the perimedullary region of the fibula in F. **J**: In some parts of the cortex, where Haversian substitution is less extensive, islands of primary bone are visible with numerous, but small longitudinal primary osteons. **K**: Cross-section of a rib of specimen SAM-PK-10026 (maximal diameter: 18.6 mm). The medullary cavity is free of bone trabeculae. **L**: Close up of the cortex in K. The primary bone is lamellar-zonal and the Haversian substitution is extensive in the mid-cortex, with several generations of secondary osteons. A good growth record is preserved in the outer cortex in some parts of the section. **M**: Dense Haversian bone in some regions of the mid-cortex. **N**: Close up on a drifting osteon with its tail of hemi-osteons and the several generations of crosscutting secondary osteons. In these regions, no remnant of primary bone is visible. Abbreviations: I Os, primary osteon; II Os, secondary osteon; CB, cortical bone; d II Os, drifting secondary osteon; Lb, lamellar bone; MZ, medullary zone; rs, resorption space.

consistent with the description of specimen SAM-PK-10074. The section presents a distinct medullary cavity, free of bone trabeculae. The deep cortex has a cancellous aspect due to an extensive bone remodeling with an imbalance towards resorption (Fig. 9K). However, the thick bone trabeculae present in the perimedullary region attest of several episodes of resorption, reconstruction and are completely secondary. Haversian bone is extensive in the mid-cortex, and in some regions of the section present up to the bone surface (Fig. 9M,N). These secondary osteons present various shapes and sizes. Surprisingly, the numerous osteocyte lacunae present in the centripetally deposited lamellar bone of the secondary osteons do not seem highly organized and fusiform, but rather round and disorganized. Some patches of primary bone are still visible in the mid-cortex of the rib and attest of the presence of a lamellar-zonal bone (Fig. 9L). Towards the periphery of the bone, the vascularization decreases until the deposition of a poorly vascularized parallel-fibered to lamellar bone with closely spaced LAGs (Fig. 9L). Several growth cycles can be observed through the cortex (Fig. 9L,M). These observations suggest that the growth of this individual had already slowed down at the time of death. However, some vascular canals pierce the bone surface (Fig. 9L) suggesting that the growth did not stop completely. In the primary periosteal bone, abundant small osteocyte lacunae are visible, as well as Sharpey's fibers. There is a clear cycle of growth visible on one side of the section (Fig. 9L). The first part seems to have been poorly vascularized and composed of a lamellar bone matrix. The second part presents small primary osteons but more importantly numerous larger secondary osteons (with several generations; Fig. 9L). In this second layer, osteocyte lacunae appear rather round and poorly organized, suggesting a faster deposition rate than in the underlying lamellar bone. Several drifting osteons are visible on this section (Fig. 9N).

DISCUSSION

Until now, the bone histology of pareiasaurs was known only for long bones and osteoderms of South African specimens identified as *Bradysaurus* and *Pareiasaurus* (Ricqlès, 1974; Scheyer and Sander, 2009), as well as isolated osteoderms of *Anthodon* and the Welgevonden pareiasaur (Scheyer and Sander, 2009). Two additional studies briefly described the histology of isolated forelimb bones (humerus, radius, ulna, scapula) of *Bunostegos akokanensis* from Niger (Looy et al., 2016) and a tibia of a Zambian specimen of *Pareiasuchus nasicornis* (Tsuji et al., 2015).

In the present study, besides re-examining the long bone histology of *Bradysaurus* and *Pareiasaurus*, we investigated for the first time the long bone histology of *Anthodon* and the Welgevonden pareiasaur. We further presented the first bone histological assessment of South African specimens identified as *Embrithosaurus* and *Pareiasuchus nasicornis*. The present work constitutes the most comprehensive survey of pareiasaur bone microstructure, in terms of generic diversity, number of specimens and variety of skeletal elements.

Preservation

The preservation of the bone microstructure appeared to be better in geologically younger pareiasaurs (*Pareiasaurus*, *Pareiasuchus*, *Anthodon*) than in the more basal and larger ones from the *Tapinocephalus* and *Pristerognathus* AZs. Interestingly, the quality of bone microstructural preservation was not always apparent at the gross macroscopic level. In general, the types of bone degradation were variable and ranged from cracks, mineral infiltrations, recrystallization, and loss of birefringence.

General Long Bone Microstructure of South African Pareiasaurs

The long bone microstructure is generally similar among the pareiasaur specimens sampled. Differences concern mostly the patterns and extent of bone remodeling between specimens or skeletal elements of the same species, or between different species. These differences are detailed below.

Generally, for most stylopodial (femur, humerus) and zeugopodial (radius, tibia, fibula) elements sampled, the medullary region is infilled by a loose to dense spongiosa consisting mostly of secondary trabeculae. The femur, humerus and tibia tend to be mostly spongy bone with thin compact cortices. The transition between the medullary region and the compact cortex is often progressive due to remodeling (imbalanced toward resorption in the perimedullary region and sometimes in most of the cortex). Resorption is usually stronger on the ventral side than on the dorsal side of these skeletal elements, thereby making the ventral side relatively more spongious. The dorsal side presents a thicker compact cortex, as already observed by de Ricqlès (1974) on a femur of *Pareiasaurus*. The fibula, radius and ribs present thicker compact cortices.

As a result of the intense perimedullary remodeling, little (if any) primary bone remains in the deep cortical regions of most limb bones and ribs. When not diagenetically altered and completely remodeled, the primary periosteal bone in the mid-cortex of pareiasaur long bones is lamellar-zonal. Zones consisting of a generally well-vascularized parallel-fibered or lamellar bone, alternate with poorly vascularized or avascular annuli and/or LAGs. When preserved, the primary cortical bone contains small, but abundant osteocyte lacunae, as well as numerous bundles of Sharpey's fibers. In some cases, Haversian substitution is so extensive that the mid-cortex consists essentially of Haversian bone. The secondary osteons tend to keep large lumens in the limb bones. In the ribs of all taxa studied, and in the fibula of *Anthodon*, Haversian bone is dense, with several generations of secondary osteons. In these cases, the secondary osteons present different shapes and orientations. Numerous instances of drifting secondary osteons (e.g., Enlow, 1962; Jasinoski and Chinsamy, 2012) are observable in these elements.

The outermost cortex of pareiasaurs sometimes presents a thick layer of avascular lamellar bone, which is interrupted by closely spaced rest lines attesting to the slower rate of growth and probably the attainment of maturity. This is best exemplified in the femur of *Pareiasaurus* sp. BP/I/5282 and the fibula of *Anthodon*

serrarius SAM-PK-10074, but was also found in other studied specimens.

Bone Microstructural Variability

Interskeletal element histovariability. Some microstructural variations exist between skeletal elements of the same individual, as well as across a single section. Thus, the bone depositional rates can differ between elements, as does the degree of remodeling, attesting to differential growth rates of skeletal elements and/or different biomechanical constraints. These are common examples of interskeletal element histovariability (Ricqlès, 1976a; Woodward et al., 2014; Padian et al., 2016). In most of the pareiasaur specimens sampled, Haversian substitution (and hence the presence of secondary osteons, or Haversian bone) is more extensive in the ribs than in limb bones, which concurs with de Ricqlès (1974) observations for pareiasaurs. This seems to also be the case for some fibulae (see *Anthodon serrarius* SAM-PK-10074, Fig. 9F–J), as compared to other, relatively larger limb bones. These observations that small skeletal elements are prone to show more Haversian substitution than larger elements agree with the hypothesis expressed by Padian et al. (2016) that larger bones grow faster and cannot accommodate as much remodeling than smaller, more slowly growing bones. Moreover, for *Bradysaurus baini* SAM-PK-5127, the degree of Haversian substitution is higher in the left fibula as compared to the right fibula (although these bones were sectioned in comparable regions). This is another example of interskeletal element variability.

Histovariability can also be important within a single section, especially in terms of the degree and type of vascularization, and the extent of bone remodeling. This was observed in various elements such as femora, ribs, and fibulae. Indeed, in all fibulae sampled, local variations in vascular organization was evident, that is, some regions of the cortex show preferential longitudinal vascular canals, while in other parts of the bone, the vascular canals have a circumferential or reticular organization. In most ribs sampled, Haversian bone is not homogeneously distributed across the section. In some regions, dense Haversian bone is present up to the periosteal surface; in others, most of the primary cortical bone is preserved, with only scattered secondary osteons.

Inter-individual histovariability. Two femora belonging to different-sized specimens identified as *Bradysaurus seeleyi* in the collections of the Iziko South African Museum (SAM-PK-9137 and SAM-PK-9165) vary in terms of the extent of Haversian substitution. Surprisingly, the largest specimen (SAM-PK-9165, femur length = 40.5 cm) shows less secondary reconstruction and more primary bone tissue in the mid- and outer-cortex as compared to the smaller specimen (SAM-PK-9137, femur length = 33.9 cm) that presents more significant secondary reconstruction with almost completely remodeled deep and mid-cortices. The extent of Haversian substitution is known to increase with age and other factors such as body size, physiological demands, or biomechanical constraints (Ricqlès, 1976a; Francillon-Vieillot et al., 1990; Mitchell and Sander, 2014). If both femora sampled indeed belong to the same species, this disparity in the extent of secondary reconstruction could reflect an age difference with the small specimen being ontogenetically older. This inconsistency between body size and apparent ontogenetic stage could be explained by inherent intraspecific variability and/or sexual dimorphism. Sexual dimorphism has been proposed for the Russian pareiasaur *Scutosaurus karpinskii*, for which two morphotypes with differential limb lengths and body sizes have been recognized (Lee, 1994b). Caution should nonetheless be exercised since differences in bone histology could also be the consequence of incorrect taxonomic identifications of pareiasaur remains from the *Tapinocephalus* AZ, and thus rather reflect inter-specific variability. Indeed, preliminary results of an ongoing taxonomic revision of pareiasaurian material from the *Tapinocephalus* AZ (Van den Brandt et al., 2016) show that specimen SAM-PK-9137 could possibly belong to the species *Nochelesaurus alexanderi* (M. Van den Brandt, 2016 pers. comm).

Discrepancy between histology and limb bone size in Middle Permian pareiasaurs (*Tapinocephalus *AZ). To some extent, bone microstructure varies among the different sized specimens of the sampled Middle Permian pareiasaurs (*Tapinocephalus* AZ). The most interesting observation is that some of the smallest individuals of our sample show ontogenetically advanced bone tissues and bone remodeling that suggest a more advanced ontogenetic stage than some larger individuals. For example, specimen Pareiasauria Indet. SAM-PK-4344, with a femur length of 26.3 cm, is among the smallest individuals represented in our sample; yet its femoral histology (having a thick layer of avascular lamellar bone with closely spaced rest lines in the outermost cortex) suggests that this animal had reached maturity and was adult at the time of its death. This is in stark contrast to the histology observed in the larger Pareiasauria Indet. SAM-PK-K322 with femoral length of 33.3 cm and *Bradysaurus seeleyi* SAM-PK-9165 with a femur length of 40.5 cm. Moreover, Haversian substitution is more advanced in the small animal SAM-PK-4344 than in the larger specimens SAM-PK-K322 and SAM-PK-9165. These findings suggest that SAM-PK-4344 was more advanced ontogenetically at the time of its death than the two larger specimens.

Intraspecific variation could perhaps explain these differences. However, it could also be the outcome of a higher taxonomic diversity of pareiasaurs than previously estimated during the Middle Permian of Southern Africa (*Tapinocephalus* AZ). Indeed, several studies have raised the issue that the taxonomy of pareiasaurs from the *Tapinocephalus* AZ needs further work. For example, in his taxonomic revision, Lee (1997a) wrote: « Some of these groups are still in considerable confusion despite the considerable efforts of many recent workers. In particular the large pareiasaurs from the *Tapinocephalus* AZ of South Africa posed a major problem, as most of the material is still very bulky and crudely prepared. As a result, I have only been able to properly examine a relatively small portion of this material ». This problem has subsequently been raised again in the literature (Jirah and Rubidge, 2014; Day et al., 2015). Moreover, a recent study described a probable new species of Middle Permian pareiasaur; suggesting that the diversity of this

group in the *Tapinocephalus AZ* is likely to have been underestimated (Cisneros and Rubidge, 2012).

It should be noted however, that although there are some doubts about the identification at the generic level of some of the specimens sampled, we are confident that they belong to the Pareiasauria. Apart from the specimens marked as Pareiasauria Indet. in Table 2, most of the others have been clearly described at the genus or species level in Lee (1997a,b) or used as such in recent studies (e.g., Day et al., 2015). Furthermore, our samples could only have been mingled with dinocephalians. It is well recognized that herbivorous dinocephalians and pareiasaurs were major constituents of the *Tapinocephalus* AZ tetrapod fauna (Smith et al., 2012), and were mostly represented by large forms with stout limb bones (Boonstra, 1969; Kemp, 2012). Both groups constituted megaherbivores, but have been hypothesized to occupy different ecological niches (Boonstra, 1969; Canoville et al., 2014). The rest of the tetrapod fauna of the *Tapinocephalus* AZ consisted of smaller non-mammalian therapsids, such as dicynodonts and therocephalians, as well as other poorly represented taxa, such as small parareptiles, pelycosaurs, and amphibians (Smith et al., 2012). Middle Permian therocephalians were carnivorous animals, with relatively long and slender limbs (Kemp, 2012) and their skeletal remains would not be easily mistaken with pareiasaurs. Moreover, their histology is different to that observed in our sample, with predominance of highly vascularized cortices and prevalence of fibrolamellar bone (and sometimes parallel-fibered bone) with limited Haversian substitution (Chinsamy-Turan and Ray, 2012; Huttenlocker and Botha-Brink, 2014). Likewise, Middle Permian dicynodonts (mostly represented by *Diictodon* and *Robertia*; Smith et al., 2012) were too small to be misidentified with pareiasaurs. *Diictodon* bone cortices are formed of well-vascularized fibrolamellar bone, with limited (if any) Haversian substitution (Chinsamy and Rubidge, 1993; Ray and Chinsamy, 2004). Early studies by Reid (1987) and de Ricqlès (1972) have shown that dinocephalian bone histology is quite different from that of pareiasaurs by having highly vascularized fibrolamellar bone in the cortices and limited Haversian substitution. We are aware of a current comprehensive assessment of South African dinocephalian bone histology (Shelton and Chinsamy, 2016). These authors' preliminary observations are congruent with previous studies (Ricqlès, 1972; Reid, 1987) and confirm that the bones of dinocephalians and South African pareiasaurs have divergent histological structures.

Discrepancy between histology and limb bone size in Upper Permian pareiasaurs. The relatively small specimen BP/I/5282 (femur length: 22 cm) already exhibits the bone histology of a mature individual with a drastic slow down of the growth and the formation of a slow deposited and poorly vascularized lamellar bone. This individual was probably mature at the time of death, but its limb bones were still growing slowly in diameter.

Pareiasuchus nasicornis SAM-PK-K6607 had been hypothesized by Lee et al. (1997) to be a juvenile, based on limb morphology. However, several histological features, such as the deposition of a layer of avascular lamellar bone interrupted by several rest lines at the surfaces of the femur and the rib, imply that the growth of this individual had already slowed down at the time of death. The important Haversian substitution in the cortices also suggests a subadult or a young-adult stage for this individual.

Finally, it has been proposed that some « dwarf » pareiasaurs, commonly found in the Upper Permian, could be juveniles of larger forms (Tsuji, 2011). However, the bone histology of the femur and the fibula of the dwarf pareiasaur *Anthodon serrarius* SAM-PK-10074 clearly indicates that this individual was mature, and an adult at the time of its death. At least 17 to 18 incremental lines were counted in the cortex of the fibula, suggesting a prolonged, punctuated period of lamellar apposition after reaching maturity. These interpretations are congruent with the osteoderm histology of the same specimen of *Anthodon* (SAM-PK-10074) studied by Scheyer and Sander (2009). The latter researchers counted up to 17 LAGs in the internal cortex of one osteoderm with decreasing spacing between the LAGs.

The histology of the rib of *Anthodon serrarius* sampled from the semi-articulated specimen BP/I/548 suggests that this individual was not mature at the time of death. In contrast with the histology of the other rib sampled from specimen SAM-PK-10026, Haversian substitution is less extensive in the deep and mi-cortex and there is no deposition of avascular lamellar bone in the outer cortex, suggesting a much younger stage for this individual.

Extent and nature of the Haversian substitution. As seen earlier at the genus level, individual differences in terms of the extent of Haversian substitution in the limb bones have been observed and we conclude that this could be linked to different ontogenetic stages. Indeed, in many tetrapod groups, Haversian substitution and the consequent formation of Haversian bone is known to increase with age (e.g., Mitchell and Sander, 2014). However, it is important to note that extensive Haversian substitution has been observed in all major morphotypes (Fig. 1A–C) of the South African pareiasaurs sampled. Indeed, the presence of numerous (yet often incipient) secondary osteons has been observed in the limb bones of large pareiasaurs from the *Tapinocephalus* AZ, but also in medium to small-sized pareiasaurs from the Upper Permian of South Africa. Although de Ricqlès (1974) did not report Haversian bone in the limb bones of *Bradysaurus*, he did document the presence of numerous secondary osteons in a *Pareiasaurus* specimen that he interpreted to be the consequence of old age and/or large body size (Ricqlès, 1974, 1976a). However, he noted that these large animals do not systematically show secondary osteons and that age was probably the main factor influencing Haversian substitution (Ricqlès, 1976a). Our findings confirm that the presence of secondary osteons is not directly linked to somatic size in pareiasaurs. Indeed we observed in our sample extensive Haversian substitution in some large basal pareiasaurs from the *Tapinocephalus* AZ (such as specimen SAM-PK-9137). However, the large pareiasaur SAM-PK-9165, which is among the largest specimens in our sample, does not show secondary osteons (at least not in the sampled region of the femur). Moreover, smaller and more derived pareiasaurs from the Upper Permian (*Pareiasaurus*, *Pareiasuchus*, *Anthodon*) tend

to show Haversian substitution in their long bones. This is especially true for *Anthodon* that shows Haversian bone with several generations of cross-cutting secondary osteons in its fibula and ribs.

The small-sized pareiasaurs from the Upper Permian have a « carapace » at the adult stage, as their body is almost completely covered by osteoderms (Lee, 1997a). However, well preserved juvenile specimens of *Elginia* have been recovered with no osteoderms (Spencer and Lee, 2000). This suggests an asynchronous development of long bones and osteoderms, with osteoderms ossifying later in ontogeny in these small derived pareiasaurs (Spencer and Lee, 2000). We could thus imagine that the growth of osteoderms has an impact on bone remodeling and Haversian subsitution in these forms, as suspected for the armored dinosaurs, such as ankylosaurs that already present secondary osteons early in ontogeny (Stein et al., 2013). Moreover, the morphology and organization of the secondary osteons in the fibula and rib of *Anthodon* is reminiscent of the organization of the Haversian bone in ankylosaurs (Stein et al., 2013). Indeed, the secondary osteons are not always longitudinal and often preserve a large lumen. Furthermore, in the rib of SAM-PK-10026, the osteocyte lacunae present in the centripetally deposited bone of the secondary osteons have a rounded and disorganized aspect. These differ from the commonly fusiform and well-organized osteocyte lacunae found in the lamellar bone of secondary osteons (Francillon-Vieillot et al., 1990; Mitchell and van Heteren, 2016). These observations suggest a relatively fast deposited secondary bone in the Haversian canals of the rib of *Anthodon*, as compared to the usually slowly formed lamellar bone of secondary osteons. This could be linked to an important phospho-calcic metabolism linked to the formation and maintenance of osteoderms (Stein et al., 2013). The observations are nonetheless based on a limited sample size and deserve further investigations that are beyond the scope of this study.

Growth Strategies

The composition of our sample (i.e., no clear ontogenetic series, limited or dubious taxonomic identifications), as well as the extensive remodeling in the cortices of most specimens has limited our interpretations about growth strategies. However, it is evident that the primary periosteal bone tissue observed in the South African pareiasaurs sampled in this study is zonal, testifying to a cyclical growth pattern. The primary bone matrix is parallel-fibered to lamellar. Our results suggest that in the first phase of growth, these animals showed a cyclical but relatively high rate of deposition (although probably not equivalent to the deposition rate of fibrolamellar bone), with the alternation of well-vascularized zones and narrow annuli and/or LAGs. At some point in ontogeny (probably coincident with the attainment of sexual maturity), growth seems to have slowed down and we observe in several specimens of all geological ages and sizes, the deposition of avascular lamellar bone with closely spaced rest lines in the outer cortex. Also, for some specimens, when the Haversian remodeling did not completely destroy the deep growth cycles, it is clear that the spacing between the growth marks decreases towards the periphery where it becomes particularly narrow. An interesting feature is that in mature individuals, appositional growth appears to continue for several years, suggesting a protracted and slow increase in bone diameter. This prolonged periosteal deposition of bone at the adult stage could contribute to the heavily built appearance of pareiasaur skeletons.

Our results concur with previous hypotheses that have suggested, on the basis of morphological and taphonomic observations, that pareiasaurs probably had a relatively short juvenile period as compared to adulthood (Spencer and Lee, 2000). The early fusion and complete ossification of girdle elements in pareiasaurs is also congruent with such a hypothesis (Turner et al., 2015).

A relatively high growth rate, at least early in ontogeny, could possibly be used in support of previous interpretations by de Ricqlès (1978) that pareiasaurs may have had intermediate physiologies as compared to other basal amniotes, with a tendency towards endothermy. The semi-erected to upright limb posture of some pareiasaurs, unique among Paleozoic Sauropsida (Sumida and Modesto, 2001; Turner et al., 2015), supports the notion that they could have had higher metabolic rates than their coeval relatives (Bakker, 1971; Ricqlès, 1978). In fact, a recent study of the limb bone morphology of *Bunostegos*, a mid-sized pareiasaur from Niger, showed that this animal had a relatively upright forelimb posture (Turner et al., 2015). This is congruent with its long bone histology that shows well-vascularized cortices with a fibrous matrix suggesting, according to Looy et al. (2016), a relatively active metabolism.

Lifestyle Adaptations

It remains difficult to draw paleoecological interpretations from the long bone microanatomy of South African pareiasaurs. In fact, most of the specimens present very spongious stylopods at the diaphyseal level (e.g., Fig. 2F). This is due to an imbalance between resorption and reconstruction during ontogeny, in favor of resorption. The periosteal cortices are thus progressively transformed into a more or less loose spongiosa during ontogeny. For most of the specimens sampled (large pareiasaur morphotypes, but also smaller ones), the femora present a spongious aspect, with a relatively thin compact cortex. This bone organization is reminiscent of the long bone inner-structure usually observed in extant pelagic marine tetrapods, such as whales or some seals (e.g., Ricqlès and Buffrénil, 2001; Canoville and Laurin, 2010), but also extinct Mesozoic marine reptiles (such as some ichthyosaurs; Ricqlès and Buffrénil, 2001). However, this bone architecture is unusual for continental tetrapods. Interestingly, pareiasaur lifestyle hypotheses have been quite varied, ranging from at least semi-aquatic to fully terrestrial (e.g., Hartmann-Weinberg, 1937; Boonstra, 1955; 1969; Benton et al., 2012; Turner et al., 2015). The taphonomy and their morphology suggest that they were not pelagic animals.

The bone microanatomy of the stylopod also differs from that of typical shallow water or bottom dweller animals such as hippos and sirenians. In fact, several studies have shown that animals living in shallow water present rather an increase in bone mass in their long bones and ribs (Ricqlès and Buffrénil, 2001; Houssaye, 2009; Canoville et al., 2016).

Recent studies using stable isotope analyses suggest that at least the large pareiasaurs from the Middle Permian were terrestrial (Canoville et al., 2014; Rey et al., 2015). Nevertheless, such femoral microanatomy is also unexpected for terrestrial extant tetrapods (Laurin et al., 2004; Quemeneur et al., 2013). Indeed, most terrestrial tetrapods tend to show rather compact cortices, with few or no perimedullary trabeculae (so a narrow and rather abrupt transitional zone between the compact cortex and the medullary cavity) and open medullary cavities (Laurin et al., 2004; Quemeneur et al., 2013). Nonetheless, a recent study has shown that large graviportal species exhibit more or less thick compact cortices in their stylopods, but their medullary cavities are always filled with a dense network of trabeculae (Houssaye et al., 2015). The extensive development of a spongiosa in the medullary region of pareiasaurs could thus be explained, at least partially, by their large body-size and body mass (at least in most basal species; Ricqlès, 1974, 1976a; Houssaye et al., 2015). However, it is difficult to explain the thin compact cortices of the femora.

It is worth mentioning that other large continental Permian tetrapods, hypothesized to have occupied equivalent ecological niches as pareiasaurs (such as some Caseidae, Maddin et al., 2008), had similar bone microanatomy. A recent study by Shelton (2014) showed that *Cotylorhynchus*, a large caseid from the Early Permian of North America, also showed completely spongious humeral diaphyses, an unusual bone architecture for such large continental animals. De Ricqlès (1974, 1976a,b) had also commented on the microanatomy of indeterminate titanosuchian (dinocephalian) from the Karoo Basin, as well as pareiasaurs such as *Bradysaurus* and *Pareiasaurus*. According to de Ricqlès (1974, 1976a,b), the presence of this spongiosa could be linked to biomechanical effects due to the large size of these animals rather than their lifestyles. It is clear that rigorous paleoecological interpretations are limited since no real modern analogue exists for these animals. Further research into this phenomenon of spongious stylopod elements in large early continental tetrapods is needed.

CONCLUSIONS

Our study has highlighted the need for an in-depth taxonomic review of pareiasaurian remains from the *Tapinocephalus* AZ. Once this is done, we would be able to better interpret the long bone histovariability observed in our Middle Permian pareiasaur samples, as well as fully understand the extent of inter- versus intra-specific variability.

Our histological observations nonetheless revealed that a small specimen from the *Tapinocephalus* AZ, which was generally considered to be a juvenile based on its small femoral size, showed a more advanced histological ontogenetic stage than much larger specimens. This therefore suggests that species diversity of the Middle Permian pareiasaurs may have been underestimated; a hypothesis already formulated in previous studies (e.g., Cisneros and Rubidge, 2012).

Furthermore, bone histology confirms that these animals experienced a relatively rapid growth early in ontogeny. The periosteal growth later slowed down (after the attainment of sexual maturity), but was prolonged for several years during adulthood.

Lifestyle adaptations of pareiasaurs remain difficult to assess based on bone microanatomy. Indeed, their stylopod microstructure is unusual for continental tetrapods, in having spongious mid-diaphyses with relatively thin compact cortices. Rigorous paleoecological interpretations are limited since no real modern analogue exists for these enigmatic early amniotes.

ACKNOWLEDGEMENTS

The authors are grateful to Iziko South African Museum, Cape Town's staff, Roger Smith (Curator), Sheena Kaal and Zaituna Erasmus (Collection Managers), as well as Bernhard Zipfel (Curator at the Evolutionary Studies Institute, former Bernard Price Institute, University of the Witwatersrand, Johannesburg) for facilitating access to the pareiasaurian material and for providing specimens for histological analyses. CHANTEX heavy Mach., Cape Town, are acknowledged for technical assistance with the high-pressure water core drilling technique used in this study. Tobias Nasterlack, Daniel Thomas, and Christen Shelton are thanked for the many stimulating discussions. The authors thank Alexandra Houssaye, John M. Rensberger, and an anonymous reviewer for their constructive comments and suggestions that improved the manuscript. They are also grateful to the editor, Tim D. Smith, for his efficient handling of their submission.

LITERATURE CITED

Bakker RT. 1971. Dinosaur physiology and the origin of mammals. Evolution 25:636–658.

Benton MJ. 2016. The Chinese pareiasaurs. Zool J Linnean Soc 177:813–853.

Benton MJ, Newell AJ, Khlyupin AYU, Shumov IS, Price GD, Kurkin AA. 2012. Preservation of exceptional vertebrate assemblages in Middle Permian fluviolacustrine mudstones of Kotel'nich, Russia: stratigraphy, sedimentology, and taphonomy. Palaeogeogr Palaeoclimatol Palaeoecol 319/320:58–83.

Benton MJ, Tverdokhlebov VP, Surkov MV. 2004. Ecosystem remodelling among vertebrates at the Permian–Triassic boundary in Russia. Nature 432:97–100.

Boonstra LD. 1932. Pareiasaurian studies. Part VII. On the hind limb of the two little-known pareiasaurian genera: *Anthodon* and *Pareiasaurus*. Ann S Afr Mus 28:429–435.

Boonstra LD. 1955. The girdles and limbs of the South African Deinocephalia. Ann S Afr Mus 42:185–326.

Boonstra LD. 1969. The fauna of the *Tapinocephalus* Zone (Beaufort beds of the Karoo). Ann S Afr Mus 56:1–73.

Botha-Brink J, Angielczyk KD. 2010. Do extraordinarily high growth rates in Permo-Triassic dicynodonts (Therapsida, Anomodontia) explain their success before and after the end-Permian extinction? Zool J Linn Soc 160:341–365.

Botha J, Chinsamy A. 2005. Growth patterns of *Thrinaxodon liorhinus*, a non-mammalian cynodont from the Lower Triassic of South Africa. Palaeontology 48:385–394.

Botha-Brink J, Smith RMH. 2012. Palaeobiology of Triassic procolophonids, inferred from bone microstructure. CR Palevol 11:419–433.

Canoville A, Buffrénil V, de, Laurin M. 2016. Microanatomical diversity of amniote ribs: An exploratory quantitative study. Biol J Linn Soc 118:706–733.

Canoville A, Laurin M. 2010. Evolution of humeral microanatomy and lifestyle in amniotes, and some comments on palaeobiological inferences. Biol J Linn Soc 100:384–406.

Canoville A, Thomas DB, Chinsamy A. 2014. Insights into the habitat of Middle Permian pareiasaurs (Parareptilia) from preliminary isotopic analyses. Lethaia 47:266–274.
Case EC. 1926. Environment of tetrapod life in the late Paleozoic of regions other than North America. Carnegie Inst Wash Publ 375: 1–211.
Castanet J, Cubo J, Margerie ED. 2001. Signification de l'histodiversité osseuse: le message de l'os. Biosystema 19:133–147.
Chinsamy-Turan A. 2005. The microstructure of dinosaur bone: Deciphering biology with fine-scale techniques. Baltimore: Johns Hopkins University Press.
Chinsamy-Turan A. 2012. Forerunners of Mammals: Radiation, Histology, Biology. Indiana University Press.
Chinsamy A, Raath MA. 1992. Preparation of fossil bone for histological study. Palaeontol Afr 29:39–44.
Chinsamy A, Rubidge BS. 1993. Dicynodont (Therapsida) bone histology: Phylogenetic and physiological implications. Palaeont Afr 30:97–102.
Chinsamy-Turan A, Ray S. 2012. Bone histology of some therocephalians and gorgonopsians, and evidence of bone degradation by fungi. In: Chinsamy-Turan A, editor. Forerunners of Mammals: Radiation, histology, biology. Bloomington: Indiana University Press. p 199–221.
Cisneros JC, Rubidge B. 2012. A new pareiasaur reptile from the *Tapinocephalus* Assemblage Zone, Middle Permian of the Karoo. Palaeont Afr 47:33.
Day MO, Ramezani J, Bowring SA, Sadler PM, Erwin DH, Abdala F, Rubidge B. 2015. When and how did the terrestrial mid-Permian mass extinction occur? Evidence from the tetrapod record of the Karoo Basin, South Africa. Proc R Soc B 282: 20150834.
Enlow DH. 1962. A study of the post-natal growth and remodeling of bone. Am J Anat 110:79–101.
Francillon-Vieillot H, Buffrénil V de, Castanet J, Géraudie J, Meunier FJ, Sire JY, Zylberberg L, Ricqlès A de. 1990. Microstructure and mineralization of vertebrate skeletal tissues. In: Carter JG, editor. Skeletal biomineralization: Patterns, processes and evolutionary trends, Vol. I. New York: Van Nostrand Reinhold. p 471–530.
Gregory WK. 1946. Pareiasaurs versus placodonts as near ancestors to the turtles. Bull Am Mus Nat Hist 86:275–326.
Gubin YM, Golubev VK, Bulanov VV, Petuchov SV. 2003. Pareiasaurian tracks from the Upper Permian of Eastern Europe. Paleontol J 37:514–523.
Hartmann-Weinberg A. 1937. Pareiasauriden als Leitfossilien. Problemy Paleontologii 2:649–712.
Houssaye A. 2009. Pachyostosis in aquatic amniotes: A review. Integr Zool 4:325–340.
Houssaye A, Waskow K, Hayashi S, Cornette R, Lee AH, Hutchinson JR. 2015. Biomechanical evolution of solid bones in large animals: A microanatomical investigation. Biol J Linn Soc 117:350–371.
Huttenlocker AK, Botha-Brink J. 2014. Bone microstructure and the evolution of growth patterns in Permo-Triassic therocephalians (Amniota, Therapsida) of South Africa. Peer J 2:e325.
Ivakhnenko MF. 1987. Permian parareptiles of the USSR. Tr Paleontol Inst Akad Nauk SSSR 223:1–159.
Jalil NE, Janvier P. 2005. Les pareiasaures (Amniota, Parareptilia) du Permien supérieur du Bassin d'Argana, Maroc. Geodiversitas 27:35–132.
Jasinoski SC, Chinsamy A. 2012. Mandibular histology and growth of the nonmammaliaform cynodont *Tritylodon*. J Anat 220:564–579.
Jirah S, Rubidge BS. 2014. Refined stratigraphy of the Middle Permian Abrahamskraal Formation (Beaufort Group) in the southern Karoo Basin. J Afr Earth Sci 100:121–135.
Kemp TS. 2012. The origin and radiation of Therapsids. In: Chinsamy-Turan A, editor. Forerunners of Mammals: Radiation, Histology, Biology. Indiana University Press. p 3–28.
Khlyupin AY. 2007. Cemetery of the Permian reptiles. Paleomir 1: 50–57.
Kordikova EG, Khlyupin AJ. 2001. First evidence of a neonate dentition in pareiasaurs from the Upper Permian of Russia. Acta Palaeontol Pol 46:589–594.
Kriloff A, Germain D, Canoville A, Vincent P, Sache M, Laurin M. 2008. Evolution of bone micranatomy of the tetrapod tibia and its use in paleobiological inference. J Evol Biol 21:807–826.
Laurin M, Girondot M, Loth MM. 2004. The evolution of long bone microstructure and lifestyle in lissamphibians. Paleobiology 30: 589–613.
Laurin M, Reisz RR. 1995. A reevaluation of early amniote phylogeny. Zool J Linn Soc 113:165–223.
Lee MSY. 1994a. The turtle's long lost relatives. Nat Hist 6:63–65.
Lee MSY. 1994b. Evolutionary morphology of pareiasaurs. Ph.D. thesis, University of Cambridge.
Lee MSY. 1996. Correlated progression and the origin of turtles. Nature 379:812–815.
Lee MSY. 1997a. A taxonomic revision of pareiasaurian reptiles: Implications for Permian terrestrial Palaeoecology. Mod Geol 21: 231–298.
Lee MSY. 1997b. Pareiasaur phylogeny and the origin of turtles. Zool J Linn Soc 120:197–280.
Lee MSY, Gow CE, Kitching JW. 1997. Anatomy and relationships of the pareiasaur *Pareiasuchus nasicornis* from the Upper Permian of Zambia. Palaeontology 40:307–355.
Looy C, Ranks SL, Chaney DL, Sanchez S, Steyer S, Smith RMH, Sidor CA, Myers TS, Ide O, Tabor NJ. 2016. Biological and physical evidence for extreme seasonality in central Permian Pangaea. Palaeogeogr Palaeoclimatol Palaeoecol 451:210–226.
Lyson TR, Bever GS, Scheyer TM, Hsiang AY, Gauthier JA. 2013. Evolutionary origin of the turtle shell. Curr Biol 23:1–7.
Lyson TR, Schachner ER, Botha-Brink J, Scheyer TM, Lambertz M, Bever GS, Rubidge BS, Queiroz KD. 2014. Origin of the unique ventilatory apparatus of turtles. Nat Commun 5:5211.
MacRae C. 1999. Life etched in stone: Fossils of South Africa. Johannesburg: Geological Society of South Africa.
Maddin HC, Sidor CA, Reisz RR. 2008. Cranial anatomy of *Ennatosaurus tecton* (Synapsida: Caseidae) from the Middle Permian of Russia and the evolutionary relationships of Caseidae. J Vert Paleontol 28:160–180.
Mitchell J, Sander PM. 2014. The three-front model: a developmental explanation of long bone diaphyseal histology of Sauropoda. Biol J Linn Soc 112:765–781.
Mitchell J, van Heteren AH. 2016. A literature review of the spatial organization of lamellar bone. CR Palevol 15:23–31.
Nasterlack T, Canoville A, Chinsamy A. 2012. New insights into the biology of the Permian genus *Cistecephalus* (Therapsida, Dicynodontia). J Vert Paleontol 32:1396–1410.
Nicolas MVM. 2007. Tetrapod biodiversity through the Permo-Triassic Beaufort Group (Karoo Supergroup) of South Africa. PhD Dissertation, University of the Witwatersrand, Johannesburg, South Africa.
Nicolas M, Rubidge BS. 2010. Changes in Permo-Triassic terrestrial tetrapod ecological representation in the Beaufort Group (Karoo Supergroup) of South Africa. Lethaia 43:45–59.
Ochev VG. 1995. Mysterious Kotel'nich. Priroda 53–59.
Ochev VG. 2004. Materials to the tetrapod history at the Paleozoic-Mesozoic boundary. In: Sun A, Wang Y, editors. Sixth Symposium on Mesozoic Terrestrial Ecosystems and Biota, Short Papers. Beijing: China Ocean Press. p 43–46.
Padian K, Lamm ET. 2013. Bone Histology of Fossil Tetrapods: Advancing Methods, Analysis, and Interpretation. University of California Press.
Padian K, Werning S, Horner JR. 2016. A hypothesis of differential secondary bone formation in dinosaurs. CR Palevol 15:40–48.
Pearson MR, Benson RB, Upchurch P, Fröbisch J, Kammerer CF. 2013. Reconstructing the diversity of early terrestrial herbivorous tetrapods. Palaeogeogr Palaeoclimatol Palaeoecol 372:42–49.
Piveteau J. 1955. Amphibiens, reptiles, oiseaux. In: Piveteau J, editor. Traité de paléontologie, Vol. 5. Paris: Masson et Cie. p 1–1113.
Quemeneur S, Buffrénil V, de, Laurin M. 2013. Microanatomy of the amniote femur and inference of lifestyle in limbed vertebrates. Biol J Linn Soc 109:644–655.

Ray S, Bandyopadhyay S, Bhawal D. 2009. Growth patterns as deduced from bone microstructure of some selected neotherapsids with special emphasis on dicynodonts: Phylogenetic implications. Palaeoworld 18:53–66.

Ray S, Chinsamy A. 2004. *Diictodon feliceps* (Therapsida, Dicynodontia): Bone histology, growth, and biomechanics. J Vert Paleontol 24:180–194.

Redelstorff R, Hübner TR, Chinsamy A, Sander PM. 2013. Bone histology of the stegosaur *Kentrosaurus aethiopicus* (Ornithischia: Thyreophora) from the Upper Jurassic of Tanzania. Anat Rec 296: 933–952.

Redelstorff R, Sander PM. 2009. Long and girdle bone histology of *Stegosaurus*: Implications for growth and life history. J Vert Paleontol 29:1087–1099.

Reid RE. 1987. Bone and dinosaurian « endothermy. ». Mod Geol 11: 133–154.

Rey K, Amiot R, Fourel F, Rigaudier T, Abdala F, Day MO, Fernandez V, Fluteau F, France-Lanord C, Rubidge BS, Smith RM, Viglietti PA, Zipfel B, Lécuyer C. 2015. Global climate perturbations during the Permo-Triassic mass extinctions recorded by continental tetrapods from South Africa. Gondwana Res. doi: 10.1016/j.gr.2015.09.008.

Ricqlès AD. 1972. Recherches paléohistologiques sur les os longs des Tétrapodes. III. Titanosuchiens, dinocéphales et dicynodontes. Ann Paléontol 58:17–60.

Ricqlès AD. 1974. Recherches paléohistologiques sur les os longs des tétrapodes.V. Cotylosaures et mésosaures. Ann Paléontol 60: 171–216.

Ricqlès AD. 1976a. Recherches paléohistologiques sur les os longs des tétrapodes.VII. Sur la classification fonctionnelle et l'histoire des tissus osseux de tétrapodes (deuxième partie). Ann Paléontol 62:71–126.

Ricqlès AD. 1976b. On bone histology of fossil and living reptiles, with comments on its functional and evolutionary significance. Linn Soc Symp Ser 3:123–151.

Ricqlès AD. 1978. Recherches paléohistologiques sur les os longs des tétrapodes. VII.—Sur la classification, la signification fonctionnelle et l'histoire des tissus osseux des tétrapodes. Troisième partie. Evolution: Considérations phylogénétiques. Ann Paléontol 64:85–111.

Ricqlès AD. 2011. Vertebrate palaeohistology: Past and future. CR Palevol 10:509–515.

Ricqlès A de , Buffrénil V de. 2001. Bone histology, heterochronies and the return of tetrapods to life in water: W[h]ere are we?. In: Mazin JM, Buffrénil V de , editors. Secondary adaptation of tetrapods to life in water. Munich: Dr Friedrich Pfeil. p 289–310.

Rubidge BS, Johnson MR, Kitching JW, Smith RMH, Keyser AW, Groenewald GH. 1995. An introduction to the biozonation of the Beaufort Group. In: Rubidge BS, editor. Biostratigraphy of the Beaufort Group (Karoo Supergroup), South African Committee for Stratigraphy, Biostratigraphic Series 1.

Ruta M, Cisneros JC, Liebrecht T, Tsuji LA, Müller J. 2011. Amniotes through major biological crises: Faunal turnover amoung parareptiles and the end-Permian mass extinction. Palaeontology 54:1117–1137.

Scheyer TM, Klein N, Sander PM. 2010. Developmental palaeontology of Reptilia as revealed by histological studies. Sem Cell Dev Biol 21:462–470.

Scheyer TM, Sander PM. 2007. Shell bone histology indicates terrestrial palaeoecology of basal turtles. Proc R Soc B 274:1885–1893.

Scheyer TM, Sander PM. 2009. Bone microstructures and mode of skeletogenesis in osteoderms of three pareiasaur taxa from the Permian of South Africa. J Evol Biol 22:1153–1162.

Shelton CD. 2014. Origins of endothermy in the mammalian lineage: the evolutionary beginning of fibrolamellar bone in the « mammal-like » reptiles. PhD Dissertation, University of Bonn, Germany.

Shelton CD, Chinsamy A. Histovariability revealed in Anteosaurid (Therapsida: Dinocephalia) limb bones. Proceedings of the 19th biennial conference of the Palaeontological Society of Southern Africa Stellenbosch, 5–8 July 2016. Palaeont Afr 51, in press.

Smith R, Rubidge B, van der Walt M. 2012. Therapsid biodiversity patterns and paleoenvironments of the Karoo Basin, South Africa. In: Chinsamy-Turan A, editor. Forerunners of Mammals: Radiation, Histology, Biology. Indiana University Press. p 31–62.

Smith RM, Sidor CA, Tabor NJ, Steyer JS. 2015. Sedimentology and vertebrate taphonomy of the Moradi Formation of northern Niger: A Permian wet desert in the tropics of Pangaea. Palaeogeogr Palaeoclimatol Palaeoecol 440:128–141.

Spencer PS, Lee MSY. 2000. A juvenile *Elginia* and early growth in pareiasaurs. J Paleont 74:1191–1195.

Stein K, Sander PM. 2009. Histological core drilling: A less destructive method for studying bone histology. In: Brown MA, Kane JF, Parker WG, editors. Methods in fossil preparation: Proceedings of the First Annual Fossil Preparation and Collections Symposium. p 69–80.

Stein M, Hayashi S, Sander PM. 2013. Long bone histology and growth patterns in ankylosaurs: Implications for life history and evolution. PLoSONE 8:e68590.

Sumida SS, Modesto S. 2001. A phylogenetic perspective on locomotory strategies in early amniotes. Am Zool 41:586–597.

Sumin DL. 2009. Hibernation as a factor responsible for preservation of the Pareiasauria in the Kotel'nich locality. In: Shishkin MA, Tverdokhlebov VP, editors. Researches on paleontology and biostratigraphy of ancient continental deposits (memories of Professor Ochev V.G.). Saratov: ÒNauchnaya KnigaÓ Publishers. p 173–176.

Tsuji LA. 2006. Cranial anatomy and phylogenetic relationships of the Permian parareptile *Macroleter poezicus*. J Vert Paleontol 26: 849–865.

Tsuji LA. 2011. Evolution, morphology and paleobiology of the Pareiasauria and their relatives (Amniota: Parareptilia). PhD Dissertation; 2010.

Tsuji LA. 2013. Anatomy, cranial ontogeny and phylogenetic relationships of the pareiasaur *Deltavjatia rossicus* from the Late Permian of central Russia. Earth Env Sci T R so 104:1–42.

Tsuji LA, Müller J. 2008. A re-evaluation of *Parasaurus geinitzi*, the first named pareiasaur (Amniota, Parareptilia). Can J Earth Sci 45:1111–1121.

Tsuji LA, Müller J. 2009. Assembling the history of the Parareptilia: Phylogeny, diversification, and a new definition of the clade. Fossil Rec 12:71–81.

Tsuji LA, Müller J, Reisz RR. 2012. Anatomy of *Emeroleter levis* and the phylogeny of the nycteroleter parareptiles. J Vert Paleonto 3245–3267.

Tsuji LA, Sidor CA, Chiba K, Angielczyk KD, Steyer J. 2015. The Permian and Triassic parareptiles of Tanzania and Zambia: Review of diversity and new life history insights provided by osteohistology. J Vert Paleontol Prog Abstracts 2015:227.

Turner ML, Tsuji LA, Ide O, Sidor CA. 2015. The vertebrate fauna of the upper Permian of Niger—IX. The appendicular skeleton of *Bunostegos akokanensis* (Parareptilia: Pareiasauria). J Vert Paleontol 35:e994746.

Tverdokhlebov VP, Tverdokhlebova GI, Minikh AV, Surkov MV, Benton MJ. 2005. Upper Permian vertebrates and their sedimentological context in the South Urals, Russia. Earth Sci Rev 69:27–77.

Valentini M, Nicosia U, Conti MA. 2009. A re-evaluation of *Pachypes*, a pareiasaurian track from the Late Permian. Neues Jahrb Geol Paläontol 251:71–94.

Van den Brandt M, Rubidge BS, Abdala F. Cranial morphology of *Embrithosaurus schwarzi* (Pareiasaur) and a taxonomic and stratigraphic reassessment of the South African Middle Permian pareiasaurs. Proceedings of the 19th biennial conference of the Palaeontological Society of Southern Africa Stellenbosch, 5–8 July 2016. Palaeont Afr 51, in press.

Voigt S, Hminna A, Saber H, Schneider JW, Klein H. 2010. Tetrapod footprints from the uppermost level of the Permian Ikakern Formation (Argana basin, western High Atlas, Morocco). J Afr Earth Sci 57:470–478.

Waskow K, Sander PM. 2014. Growth record and histological variation in the dorsal ribs of *Camarasaurus* sp. (Sauropoda). J Vert Paleontol 34:852–869.

Woodward HN, Horner JR, Farlow JO. 2014. Quantification of intraskeletal histovariability in *Alligator mississippiensis* and implications for vertebrate osteohistology. PeerJ 2:e422.